Seismology : introduction

By far our most important tool for probing the $\oplus$'s interior. Many different "types" of seismology, all share same basic picture, namely

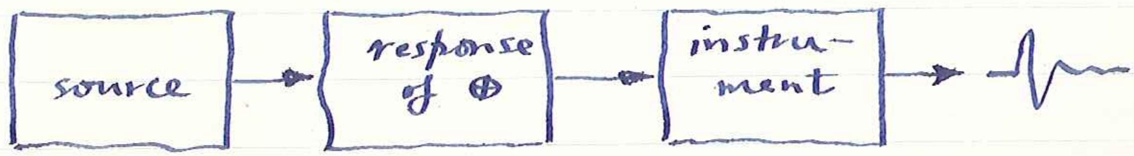

The source may be natural (earthquakes) or artificial (explosions, nuclear, quarry blasts, or specially for seismic exploration, Vibroseis®)

It generates waves which propagate through the $\oplus$ or from an alternative point of view it excites free oscillations of Earth. Response of $\oplus$ to source can be considered linear since seismic displacements are quite small.

The instrument has its own response, hopefully if well designed, linear also. Also its effect is presumably known (instrument response calibrated).

General program: given 1 or N wiggly lines infer elastic and anelastic properties of ⊕ and infer nature of seismic source if it is a quake.

Linear elasticity: a continuum approach

For seismological purposes perfectly elastic and isotropic materials may be characterized by three parameters which may be functions of position within the ⊕

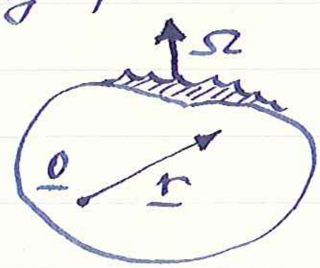

1. mass density $\rho(\underline{r})$ [gm / cm^3]

typical values:

granite: $\rho = 2.7$

basalt: $\rho = 2.9$

peridotite ~~dunite~~: $\rho = 3.3$ (lots of Mg)

mean ⊕: $\bar{\rho} = 5.517$

Fe: $\rho = 7.9$

There are also two elastic parameters which we have already introduced

2. bulk modulus or incompressibility $\kappa(\underline{r})$: a measure of ability to withstand compression

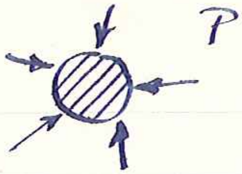

sample under
<u>initial</u> pressure
P, volume V
(need not be spherical
for defn * but if
so it is easy to visualize

augment pressure
by dP,
volume <u>change</u>
dV (negative)
i.e. new volume
is V + dV

deformation (purely radial).

Then:

$$\boxed{{}^{*}\kappa = \left[-\frac{1}{V}\left(\frac{dV}{dP}\right)\right]^{-1}}$$

this makes $\kappa > 0$

this form

or rewritten

$$\boxed{dP = -\kappa\,(dV/V)}$$

incremental change in pressure

fractional change in volume

	GPa	κ (dyne / cm^2)
granite	55	$5.5 \cdot 10^{11}$
basalt	75	$7.5 \cdot 10^{11}$
peridotite ~~dunite~~	100	$10. \cdot 10^{11}$
steel	170	$17. \cdot 10^{11}$
H_2O	2	$0.2 \cdot 10^{11}$

in general the denser a material the more incompressible

3. <u>rigidity</u> or <u>shear modulus</u>
$\mu(\underline{r})$ also dyne/cm^2 :
a measure of ability to withstand <u>shear</u> stress, a thought experiment

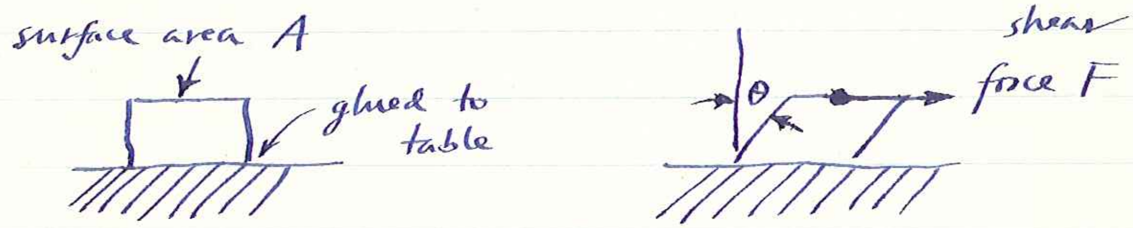

The block is sheared, angle θ is a measure of shear

$$F/A = 2\mu\theta$$

conventional to put 2 here

shear force per unit area

shear of block

$$\boxed{\mu = \frac{F/A}{2\theta}}$$

ratio of shear force to shear deformation just as K is ratio compressive force to compressive deformation

$$\boxed{F/A = 2\mu\theta}$$

A <u>fluid</u> by definition has <u>zero rigidity</u>.

	μ (dyne/cm^2)	
granite	20	$2 \cdot 10^{11}$
basalt	40	$4 \cdot 10^{11}$
peridotite ~~dunite~~	80	$8 \cdot 10^{11}$
	↑ GPa	

These are "typical" values of geological materials at 1 atmosphere.
A given material becomes more rigid and more incompressible (and of course denser) when the initial pressure acting on it is increased.
This accounts for most but not all of the increase with depth of ρ, κ and μ in the mantle.

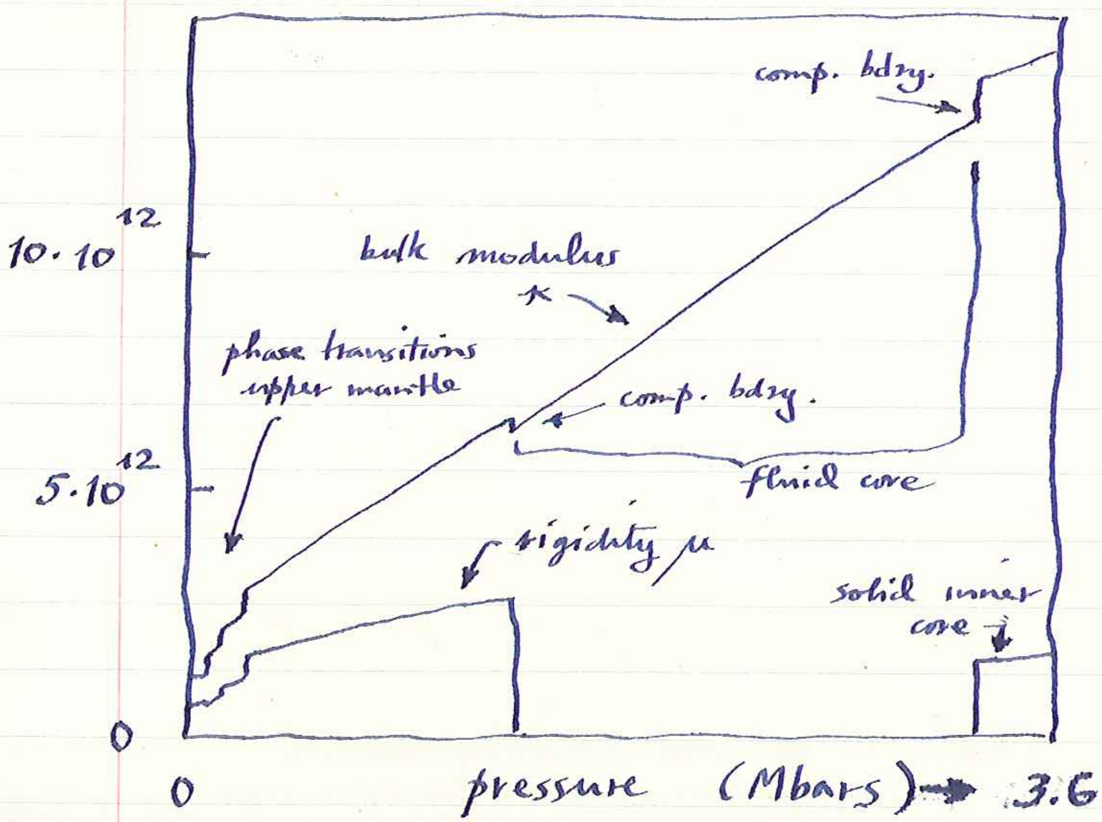

1 Mbar $= 10^6$ bars
1 bar $= 10^6$ dyne/cm^2
1 Pa $= 10$ dyne/cm^2

A major goal of seismology, esp. global seismology, is the determination of variation of $\rho(r)$, $\kappa(r)$ and $\mu(r)$ with depth in ⊕. Will discuss how this is done in detail.

Isotropic materials are those which "look the same" or more accurately "respond the same" in all directions. Minerals are typically anisotropic but rocks are aggregates of randomly oriented minerals and thus are usually reasonably isotropic. Evidence for crustal and upper mantle anisotropy exists but as first approximation we'll assume isotropic. A perfectly elastic ⊕ has only 2 independent elastic parameters, 1 for compression and one for shear.

There are other related, not independent parameters, e.g. Lamé's parameters λ and μ. the former defined by

$$\boxed{\lambda = \kappa - \frac{2}{3}\mu}$$

units again dyne/cm^2

Poisson's ratio ν : dimensionless

stretch a rod

$$\boxed{\nu \equiv \frac{\text{decrease in either lateral dimension}}{\text{increase in length}}}$$

Can show that $\boxed{\nu = \dfrac{\kappa - 2/3\,\mu}{2(\kappa + \frac{1}{3}\mu)}}$

fluid : $\nu = 1/2$

For most common materials $\nu \sim 1/4$, corresponds to $\lambda = \mu$ or $\kappa = 5/3\,\mu$

Note from above tables this true for granite, basalt, etc.

Seismic wave propagation

In an isotropic and homogeneous material : $\kappa(\underline{r}) = \kappa$

$$\mu(\underline{r}) = \mu$$
$$\rho(\underline{r}) = \rho$$

two types of seismic waves can propagate.

1. <u>P waves</u> (P stands for <u>prim</u>ary historically, as these are the first to arrive after an earthquake, can also stand mnemonically for pressure)

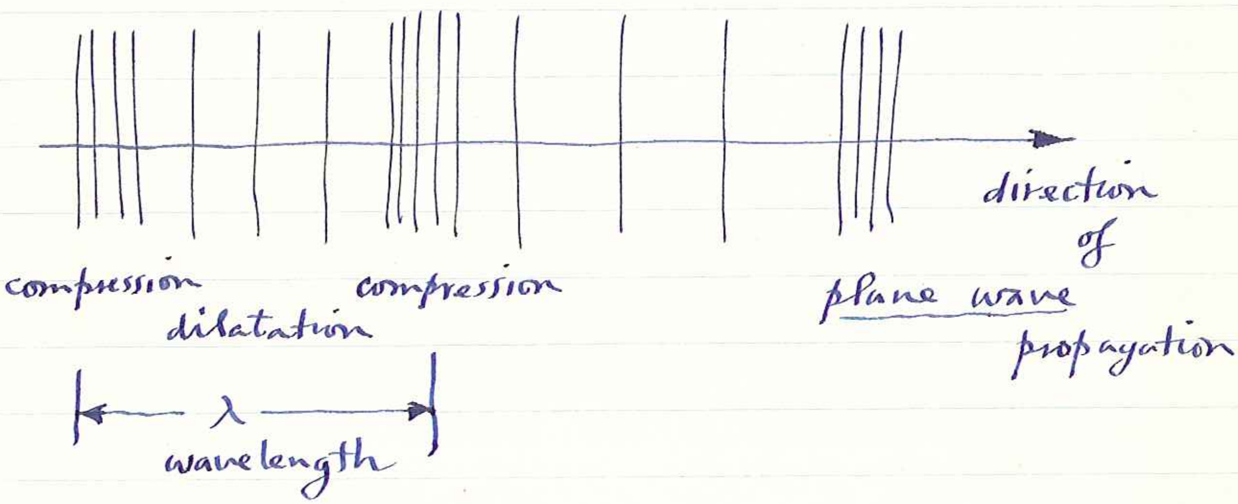

These are waves of compression and dilatation, although shearing motions are involved also. These are basically <u>sound waves</u>
The speed of P waves is

$$\boxed{\alpha = v_p = \left(\frac{\kappa + \frac{4}{3}\mu}{\rho} \right)^{1/2}}$$

Depends on both κ and μ as both compression and shear are involved. These can propagate in a <u>fluid</u> ($\mu = 0$) e.g. in air or H_2O (sound waves)

Particle motions in a shear wave are parallel to the direction of propagation

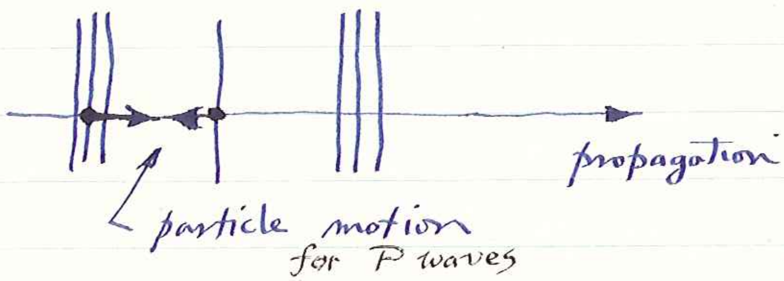

2. S waves (stands for secondary, also mnemonically for shear), pure shear, speed depends only on rigidity μ

$$\boxed{\beta = v_s = (\mu/\rho)^{1/2}}$$

Particle motions are transverse or $\perp$ to the direction of propagation

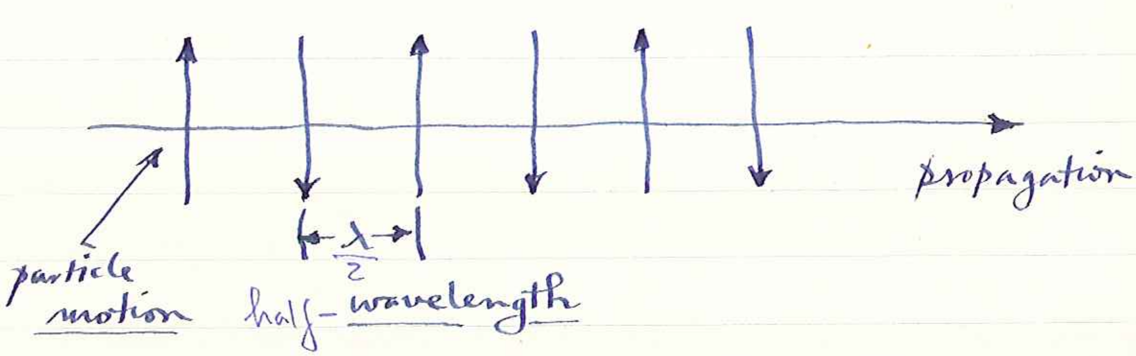

The orientation of the particle motion is referred to as the polarization.

Note that both K and μ must by defn. be positive:

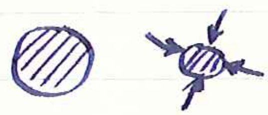

volume must decrease when pressure applied

block must shear in direction shown for force F

Thus α must be greater than β for any (stable) material. For a Poisson solid $\lambda = \mu$ or $\nu = 1/4$

$$\alpha = \sqrt{3}\,\beta = 1.732\,\beta .$$

$\alpha \approx 1.7\beta$

This a good rule of thumb, P waves about 1.7 times faster than shear waves.

	α (km/s)	β (km/s)
granite	6.0	3.6
basalt	7.0	3.8 – 3.9
peridotite ~~dunite~~	7.9 – 8.1	4.6

this, again, at 1 atm.

Kinematic properties of plane waves:

The variation with time and space of, say, particle displacements in a wave (or pressure in a P wave) is of the form (for monochromatic wave)

$$\boxed{A \cos(\omega t - kx)}$$

- A: amplitude
- k: wavenumber (radians/km)
- ω: angular frequency of wave (radians/sec)

Snapshot at time t:

period $T = \frac{2\pi}{\omega}$

wavelength $\lambda = \frac{2\pi}{k}$

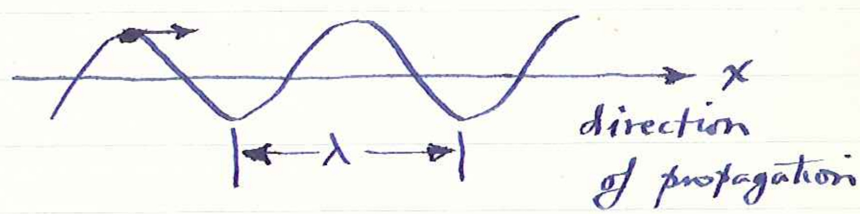

The speed of wave crests (• in picture) called the phase speed is

$$\boxed{v = \omega / k = \frac{\lambda}{T}}$$

v: either α for P waves or β for S waves

The <u>wavelength</u> $\boxed{\lambda = 2\pi / k \quad \text{in km.}}$

Can also write in form

$$A \cos \omega \underbrace{(t - x/v)}$$

this takes the same value at points $x = vt$, this the speed of wave crests

At a fixed x, the <u>variation in time</u> also sinusoidal, frequency ω.

variation with t
at fixed posn. (e.g. at a seismic station)

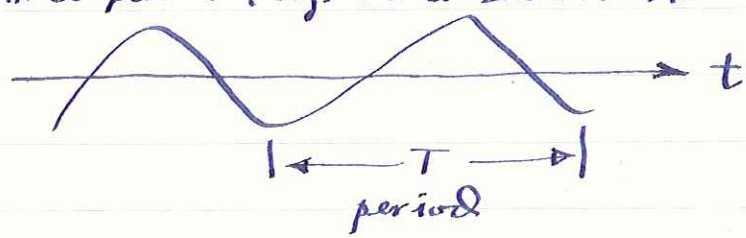

$$\boxed{\text{period} \quad T = 2\pi / \omega}$$

Can also write speed in terms of λ and T, viz

$$\boxed{c = \lambda / T}$$

peridotite (upper mantle)

Consider ~~granite~~, e.g. $\alpha =$ ~~6.0~~ 8.0 km/sec

freq (Hz)	period (sec)	wavelength λ_P	application
~~10~~	~~0.1~~	~~600 m~~	~~prospecting 10 Hz and up~~
1	1	8 ~~6~~ km	short period WWSSN
0.1	10	80 ~~60~~ km	long period WWSSN

In the seismology labs we'll be looking at waves in the range 1–10 sec with λ in the range 6 – 60 km. Then we'll look at longer wavelength surface waves.

For a given period T or frequency ω S waves are <u>shorter</u> wavelength than P waves. We'll look at both in the lab.

$$\lambda = cT$$

$$\lambda_P / \lambda_S = \alpha / \beta \sim 1.7$$

S waves are ~1.7 times shorter wavelength

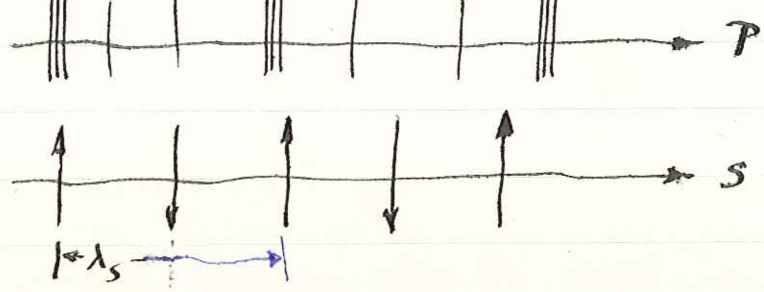

skip this

Anelasticity and damping of seismic waves

No real material is perfectly elastic. If a block were perfectly elastic it would require no net work to flex it back and forth with a harmonically varying force

Any real block will dissipate energy due to internal friction. On a microscopic level might be, e.g. grain boundary friction or bowing of pinned dislocations. The dissipated energy appears as heat in the block. When the block is deformed there is stored elastic energy in it. The intrinsic Q of a material is defined by

$$\boxed{Q = 4\pi \frac{\text{average stored energy}}{\text{energy dissipated per cycle}}}$$

Thus $4\pi Q^{-1}$ is the percentage of the average energy dissipated per cycle. Dimensionless.

In the above experiment the deformation is pure shear and the Q is called the shear Q, usually denoted by Q_μ.

In principle energy can also be dissipated in pure compression

There are thus for an isotropic material two intrinsic Q's

$$\boxed{\begin{array}{ll} Q_\mu : & \text{shear} \\ Q_\kappa : & \text{bulk} \end{array}}$$

There is some (not completely convincing) evidence that Q_κ in the mantle is finite, namely the Q's of the radial modes which have very little shear.
Reason: bulk $\frac{dV}{V} \Rightarrow$ shears on a grain-size scale.

But for a first approx. it suffices to assume that:

$$\boxed{Q_\kappa(\underline{r}) = \infty \quad \text{throughout } \oplus}$$

The shear Q_μ can vary in the $\oplus$ (must be ∞ in the fluid core where there is no shear), depends strongly on temp. T, dislocation density, impurities, etc.

Thus 4 parameters seismology seeks to determine and which characterize the middle box completely:

source $\longrightarrow$ $\boxed{\oplus\text{'s response}}$ $\longrightarrow$ instrument

$$\left.\begin{array}{ll} \rho(\underline{r}) & \text{density} \\ \kappa(\underline{r}) & \text{bulk modulus} \\ \mu(\underline{r}) & \text{rigidity} \end{array}\right\} \quad \text{these three can be replaced by others, common to use instead}$$

$$\begin{array}{ll} Q_\mu(\underline{r}) & \text{shear } Q \end{array}$$

$$\rho(\underline{r}), \quad \alpha(\underline{r}), \quad \beta(\underline{r})$$

$$\left(\alpha^2 = \frac{\kappa + 4/3\,\mu}{\rho}, \quad \beta^2 = \frac{\mu}{\rho}\right)$$

From a rather abstract point of view this is all seismology can ever tell us about the ⊕, the middle box, the variation of these four parameters as fcn. of posn. within the ⊕. The principal variation is with depth but there are also <u>lateral differences</u> which are of interest, e.g. that between continents and oceans, subducted slabs, etc.

<u>Attenuation of seismic waves</u>: a consequence of finite Q.

In a non-attenuating medium a plane wave propagates with no diminution of its amplitude

$$A \cos(\omega t - kx)$$

amplitude

A trick for determining the amplitude decay which we shall not prove but merely assert is the following:

1. write signal in the form

$$\mathrm{Re}\left[A e^{i(\omega t - kx)} \right]$$

$$= \mathrm{Re}\left[A e^{i\omega(t - x/v)} \right]$$

2. replace the real moduli κ and μ by

$$\boxed{\kappa \to \kappa(1 + i/Q_\kappa)}$$

$$\boxed{\mu \to \mu(1 + i/Q_\mu)}$$

i.e. $1/Q_\mu$ is the <u>imaginary part</u> of the shear modulus

Consider first an <u>S wave</u>, velocity $\beta = (\mu/\rho)^{1/2}$.

It is essentially always a good approximation to assume that $Q_\mu \gg 1$, fails only in very wet sediments, etc., but a good approx. for any igneous rock, for mantle, etc.

$$\beta \to \left[\frac{\mu(1+i/Q_\mu)}{\rho} \right]^{1/2}$$

$$= \beta (1+i/Q_\mu)^{1/2}$$

$$\approx \beta (1+i/2Q_\mu)$$

$$\boxed{\beta \to \beta(1+i/2Q_\mu)}$$

Thus $\quad t - \frac{x}{\beta} \to t - \frac{x}{\beta(1+i/2Q_\mu)}$

$$\approx t - \frac{x}{\beta} + i \frac{x}{\beta 2Q_\mu}$$

$$\mathrm{Re}\left[A e^{i\omega(t - x/\beta)} \right] \to$$

$$A e^{-\frac{\omega x}{2\beta Q_\mu}} \cos(\omega t - kx)$$

decay of amplitude of wave with distance, can also write as

since $\frac{\omega}{\beta} = k = \frac{2\pi}{\lambda}$

$$\boxed{A \exp\left(-\frac{\pi}{Q_\mu}\frac{x}{\lambda}\right) \cos(\omega t - kx)}$$

$$\boxed{\text{decays by } 1/e \text{ after a propagation distance } x = (Q_\mu/\pi)\lambda\text{, i.e. } Q_\mu/\pi \text{ wavelengths}}$$

~~Q_μ wavelengths~~

There is some evidence that Q_μ goes up above 1 Hz; important for detection of "decoupled" explosions.

A typical value for Q_μ in the mantle is $Q_\mu \sim 300$. A 10 s wave with an S wave velocity of 6 km/sec in mantle and a λ of 60 km will thus travel about 6000 km $\sim$ radius of $\oplus$ before attenuating by $1/e$. A 1 s wave will only go 600 km, higher frequency waves are attenuated more quickly.

Now consider a P wave (with $Q_\kappa = \infty$):

$$\alpha \to \left[\frac{\kappa + \frac{4}{3}\mu(1 + i/Q_\mu)}{\rho} \right]^{1/2}$$

$$= \left[\frac{(\kappa + 4/3\,\mu)\left(1 + \frac{4/3\,\mu}{\kappa + \frac{4}{3}\mu}\,\frac{i}{Q_\mu}\right)}{\rho} \right]^{1/2}$$

$$\approx \alpha \left(1 + i\,\frac{4/3\,\mu}{2(\kappa + \frac{4}{3}\mu)}\,Q_\mu^{-1}\right)$$

$$\boxed{\alpha \to \alpha\left[1 + i/2Q_\mu\,(3\alpha^2/4\beta^2)\right]}$$

Q_μ also called Q_β in study of body wave attenuation.

One defines for P waves

$$\boxed{Q_\alpha = (3\alpha^2/4\beta^2)\, Q_\beta}$$

ratio of Q for P waves to Q for S waves if $Q_K = \infty$

Then:

S waves: $$A \exp\left(-\frac{\omega x}{2\beta Q_\beta}\right) \cos(\omega t - kx)$$
$$= A \exp\left(-\frac{\pi x}{Q_\beta \lambda}\right) \cos(\omega t - kx)$$

P waves: $$A \exp\left(-\frac{\omega x}{2\alpha Q_\alpha}\right) \cos(\omega t - kx)$$
$$= A \exp\left(-\frac{\pi x}{Q_\alpha \lambda}\right) \cos(\omega t - kx)$$

For a Poisson solid $\alpha^2 = 3\beta^2$ and

$$\boxed{Q_\alpha = \frac{9}{4} Q_\beta = 2.25\, Q_\beta}$$

Q_α is bigger than Q_β because deformation in an S wave is pure shear while that in an S wave only partly shear.

In a given distance x how much more rapidly does an S wave of a given frequency decay?

Two reasons for difference:

1. $Q_\alpha > Q_\beta$
2. λ for S waves shorter because they are slower and $\therefore \exists$ more stress cycles in a given path.

If we write amplitude decay as

$A e^{-\gamma x}$, then:

same

$$\gamma_P = \frac{\omega}{2\alpha Q_\alpha}, \quad \gamma_S = \frac{\omega}{2\beta Q_\beta}$$

$$\boxed{\gamma_S / \gamma_P = \frac{\alpha Q_\alpha}{\beta Q_\beta} = \frac{3}{4}\frac{\alpha^3}{\beta^3}}$$

For a Poisson solid $\gamma_S / \gamma_P \sim 3.9$

S waves should decay ~ 4 times as fast as P waves over a given path.

Seismic body waves:

The subject we shall study in greater detail is global seismology, used to infer global properties of $\oplus$ and nature of natural sources, earthquakes.

Large nuclear explosions have also been employed in travel time studies.

The most useful way of analyzing and comprehending seismic motion in range $\lesssim 40\,s$ is as propagating body waves.

Consider first a point source earthquake in an ∞ homogeneous medium. Energy spreads out from the hypocenter

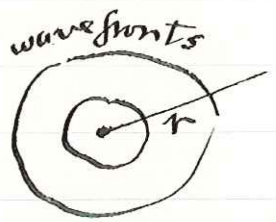

both P and S waves will (in gen'l) be generated, spread out at speeds α and β, respectively

The wave equation for the P waves can be shown to be

$$\boxed{\begin{array}{l} \nabla^2 \theta(\underline{r}, t) = \dfrac{1}{\alpha^2}\, \partial_t^2\, \theta(\underline{r}, t) \\ \qquad \text{where } \theta \equiv \nabla \cdot \underline{s}(\underline{r}, t), \\ \qquad \text{the dilatation} \\ \star \quad \text{Same eqn for pressure } p(\underline{r}, t) \end{array}}$$

This valid everywhere except at the source $r = 0$. Recall this in homog. medium :

$$\alpha = \left(\frac{\kappa + 4/3\,\mu}{\rho} \right)^{1/2} = \text{const.}$$

General solution of $\star$ is

$$\theta(\underline{r}, t) = \frac{1}{r} f(r - \alpha t) + \frac{1}{r} g(r + \alpha t),$$

f and g arbitrary fcns

$g(r + \alpha t)$ ~~outward~~ inward traveling, non-physical

Check : for a function independent of θ, ϕ we have

$$\boxed{\nabla^2 = \frac{1}{r^2}\, \partial_r\, (r^2\, \partial_r)} \quad \frac{1}{r^2} \frac{\partial}{\partial r}\left(r^2 \frac{\partial}{\partial r} \right)$$

$$\nabla^2 \left[\frac{1}{r} f(r - \alpha t) \right] =$$

$$\frac{1}{r^2} \frac{\partial}{\partial r} (rf)' = \frac{1}{r^2} \frac{\partial}{\partial r} (rf' - f)$$

$'$ and ∂_r are same

Here f' = derivative of f

$$= \frac{1}{r} f'' + \frac{1}{r^2} f' - \frac{1}{r^2} f' = \frac{1}{r} f''$$

equal, checks

And $\frac{1}{\alpha^2} \partial_t^2 \left[\frac{1}{r} f(r - \alpha t) \right] = \frac{1}{r} f''$

Thus the general solution is

$$\boxed{\theta(\underline{r}, t) = \frac{1}{r} f(r - \alpha t)}$$

travels outward with velocity α

amplitude falls off like $\frac{1}{r}$.

The $\frac{1}{r}$ falloff called <u>geometrical attenuation</u>.

Simple physical interpretation. The energy of wave motion is

$$\boxed{\text{energy} \sim (\text{amplitude})^2}$$

Thus energy $\sim \frac{1}{r^2}$.

Geometrical attenuation thus just a consequence of energy conservation. Consider two spherical surfaces, radii r_1 and r_2. The only source of radiated energy at the hypocenter.

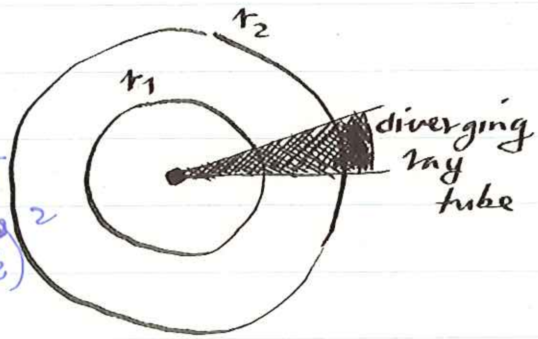

energy × area = const

$E_1 (4\pi r_1^2) = E_2 (4\pi r_2^2)$

$$\frac{E_2}{E_1} = \left(\frac{r_1}{r_2}\right)^2$$

Thus the total energy passing thru the 2 spheres must be the same. Ratio of areas is $(r_2/r_1)^2$. Thus ratio of seismic energy / unit area in the wavefronts must be $(r_1/r_2)^2$, or

$$\boxed{\text{energy / unit area} \sim \frac{1}{r^2}}$$

Same law for intensity of light emitted by a lightbulb, for example. We now know essentially everything about wave propagation in homogeneous media:

1. two types of waves, P and S, velocities α and β.
2. waves generated by point sources suffer geometrical

<u>attenuation</u>, amplitude $\sim \frac{1}{r}$,
energy $\sim \frac{1}{r^2}$.

3. <u>anelasticity</u> causes further <u>anelastic attenuation</u> $\sim e^{-\alpha r}$, where $\gamma_S \to \alpha_S / \alpha_P \leftarrow \gamma_P = \frac{3}{4}(\alpha/\beta)^3 \sim 3.9$. The region between r_1 and r_2 <u>absorbs</u> this energy. Actually, $\gamma = \frac{\omega}{2vQ}$.

should call this γ not α

We previously discussed anelastic attenuation in context of <u>plane waves</u>

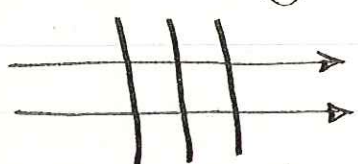

wavefronts

Point sources generate <u>spherical</u> waves but several wavelengths from the source these appear to be <u>locally</u> plane and our reasoning about anelastic attenuation is valid.

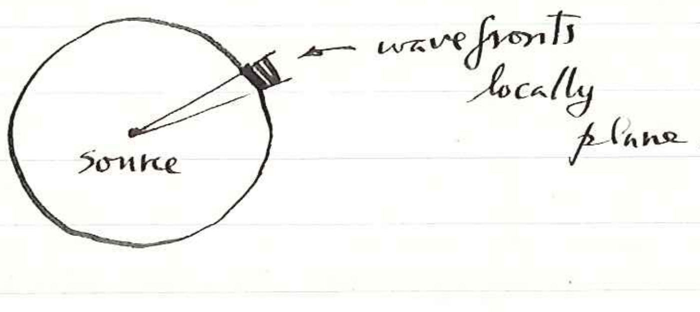

Now consider an earthquake in the Earth, <u>not</u> homogeneous, α and β functions of radius.

Near the source can think of as essentially locally homogeneous. Thus wavefronts ~ spherical: But then what happens? A very good approximation is provided by the theory of <u>geometrical optics</u> or <u>seismic ray theory</u>.

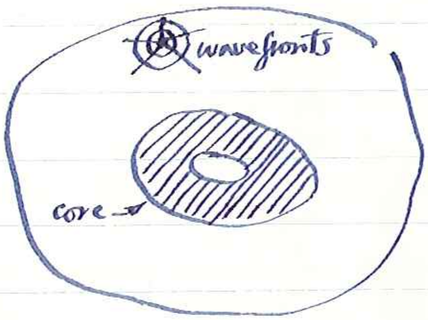

Near the source can think of energy as propagating along straight <u>rays</u> with velocity either α or β. After time t disturbance confined to sphere of radius αt or βt

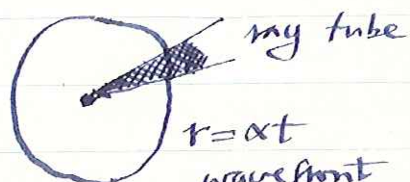

The amplitude falls off like

$$\boxed{\text{amplitude} \sim (\text{energy})^{1/2} \sim \frac{1}{r} \sim \frac{1}{\sqrt{\text{area of ray tube}}}}$$

Geometrical optics provides the generalization of this to inhomogeneous media.

Conditions for validity of geometrical optics are: scale length L of changes in $\kappa(\underline{r})$, $\mu(\underline{r})$ or $\rho(\underline{r})$ must be much greater than λ = wavelength of waves

$$\boxed{\lambda \ll L}$$

Under these conditions propagation still along rays, that along a given ray essentially independent of other rays.

"Typical" seismic wavelength $\alpha \sim 8$ km/s upper mantle, long-period body wave $T \sim 10$ s, $\lambda \sim \alpha T \sim 80$ km.

Ray approximation will be good almost everywhere since changes in ρ, κ, μ are small on this scale, except for a few sharp discontinuities, e.g. Moho and core-mantle boundary, to which will return later. An extension of geometrical optics allows us to deal simply with these also.

The two <u>laws</u> of <u>ray</u> <u>theory</u> are:

1. <u>Fermat's</u> <u>principle</u> of stationary time: of all possible paths between 2 fixed points the actual ray paths are those for which the travel time achieves a stationary value (usually but not always a minimum)

To be more specific, say $v(\underline{r})$ is given everywhere in space and say that $\lambda \ll L$.

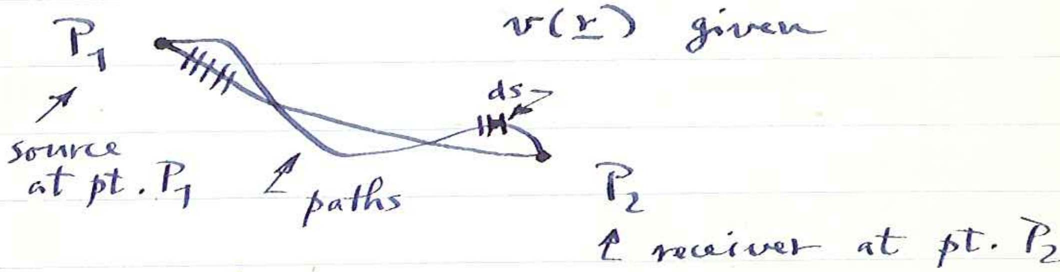

Now parameterize paths by <u>arclength</u> s along path. Then velocity of wavefronts along a possible path is $v(s)$. The <u>time</u> to travel a path is

$$\boxed{T = \int_{P_1}^{P_2} \frac{ds}{v(s)}}$$

in a sense, $\frac{\delta T}{\delta \text{path}} = 0.$

$$\boxed{\begin{array}{l}\underline{\text{Fermat's}}\ \underline{\text{principle}} :\quad \delta T = 0 \\ \text{for a small change in the path.}\end{array}}$$

Note: this agrees with what we know for a <u>homogeneous</u> medium, $v(\underline{r}) = v = \text{const.}$

$$T = \int_{P_1}^{P_2} \frac{ds}{v} = \frac{1}{v} \underbrace{\int_{P_1}^{P_2} ds}_{\text{arclength}}$$

$$T = v \times \text{arclength}$$

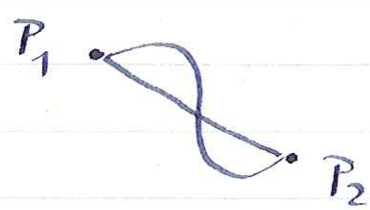

Path with <u>shortest</u> arclength is <u>straight line</u>: rays are straight lines in homog. media, radiate straight outward from source

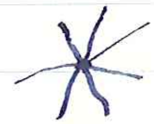

In this case the stationary value is a <u>minimum time path</u>.

2. Geometrical attenuation law:
This law governs the wave amplitude along a ray in the absence of attenuation.

Fermats' principle determines the paths and the propagation times along them.

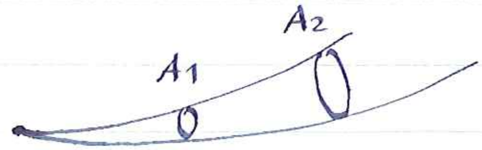

A_i = cross-sectional area of a ray tube or bundle of rays

The geometrical attenuation law states that:

$$\boxed{\frac{\text{amplitude at 2}}{\text{amplitude at 1}} = \left(\frac{A_1}{A_2}\right)^{1/2}}$$

Energy ~ 1/area
Amplitude ~ $1/\sqrt{\text{area}}$

This agrees with and generalizes 1/r falloff in homog. media.

The <u>additional attenuation</u> due to anelasticity can also be easily calculated in the ray approximation.

skip this

For a straight ray in a <u>homogeneous</u> medium we have seen it is

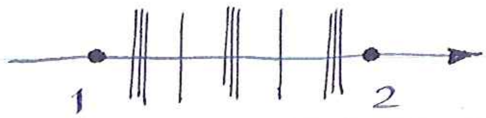

frequency (rad/s) of wave

distance

$$\frac{\text{amplitude at 2}}{\text{amplitude at 1}} = e^{-\frac{\omega x}{2vQ}}$$

either Q_α or Q_β

either α or β

The obvious generalization of this if both $v(\underline{r})$ and $Q(\underline{r})$ are variable is

$$\frac{\text{amplitude at 2}}{\text{amplitude at 1}} = e^{-\omega \int_{P_1}^{P_2} \frac{ds}{2vQ}}$$

It is conventional to call the integral above

$Q(\underline{r})$ fcn. of posn., e.g. LVZ is a low Q zone as well

$$\boxed{t^* \equiv \int_{P_1}^{P_2} \frac{ds}{2vQ}}$$

If $Q(\underline{r}) = Q$, constant, then $t^* = T/2Q$ where T = travel time.

The total expression for the variation in amplitude along a ray is thus

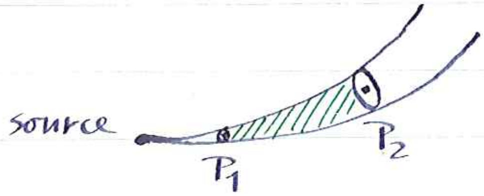

this energy is absorbed within the shaded region

$$\frac{\text{ampl. at } 2}{\text{ampl. at } 1} = \left(\frac{\text{area } A_1}{\text{area } A_2}\right)^{1/2} e^{-\omega t^*}$$

frequency-independent geometrical attenuation

anelastic attenuation affects high frequencies much more strongly, t^* typically a few seconds.

e.g. if $T \sim 30$ min (teleseismic S) and $Q_\beta \sim 300$, $t^* \sim 3$ secs.

S waves:

T (sec)	$e^{-\omega t^*}$
60	0.73
10	0.15
1	6.6×10^{-9}

very sharp cutoff.

Discontinuities: what happens when a wave encounters a sudden discontinuity, e.g. the core-mantle boundary?

An extension of ray theory is applicable in this case subject to the same proviso that $\lambda \ll L$ where now $L \approx$ radius of curvature of boundary.

Far from the source, wavefronts appear locally plane. If on scale of waves the bdry appears to be essentially locally plane as well,

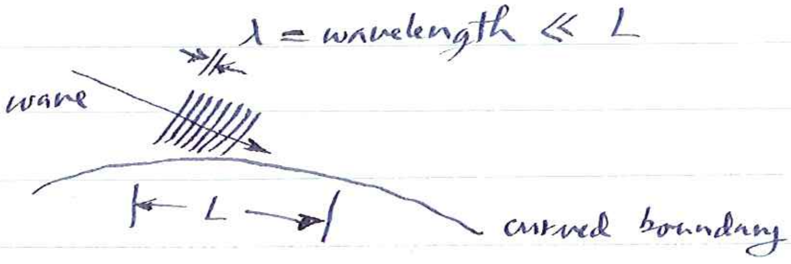

Can then model as <u>plane wave</u> impinging on a plane boundary

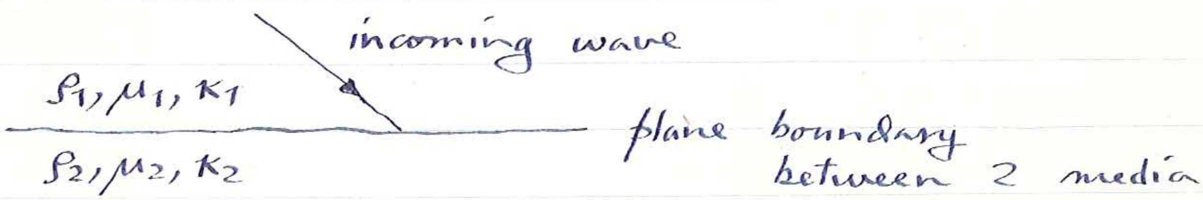

Now becomes important to consider <u>polarization</u> of <u>S wave</u>.
<u>Nomenclature</u>:

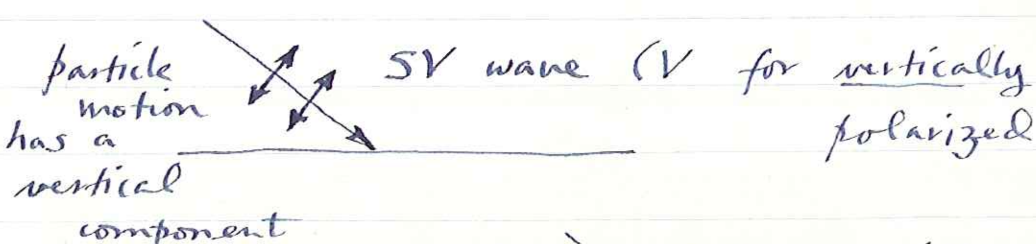

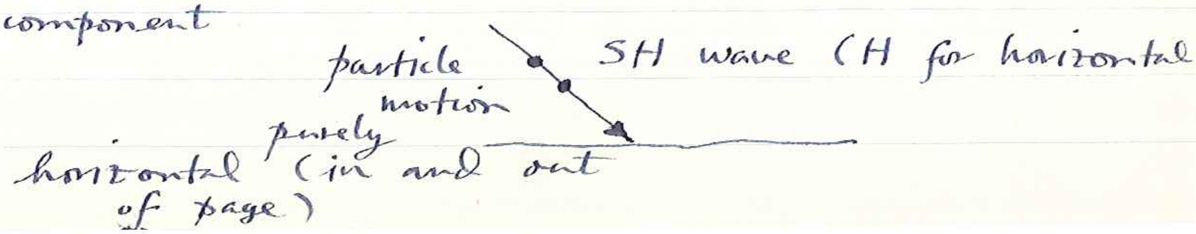

Can also have incident P wave

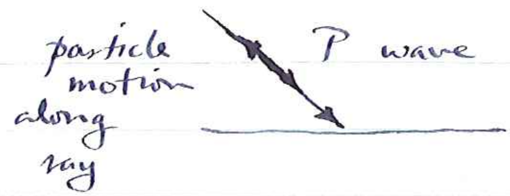

Can also impinge on bdry from below:

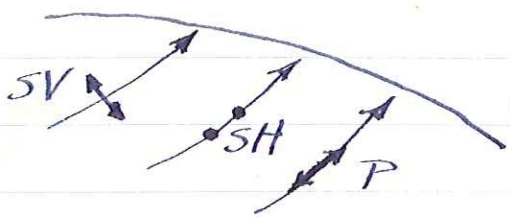

⊕ surface, e.g.

A wave incident on a bdry can, in general, give rise to both a transmitted and reflected wave

Incident SH can only generate reflected and transmitted SH.

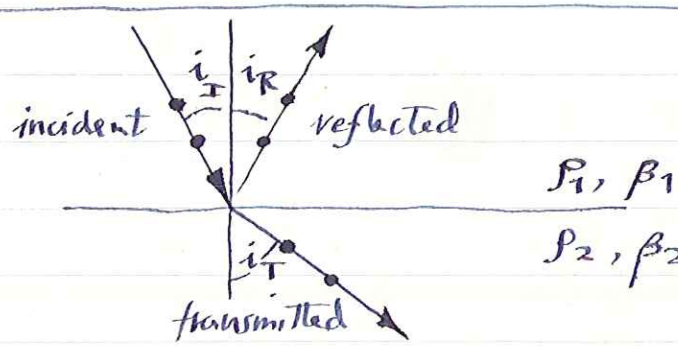

This picture is appropriate if β_2 is greater than β_1

P and SV waves are however <u>coupled</u> at interfaces, thus, e.g. an <u>incident P wave</u> can generate

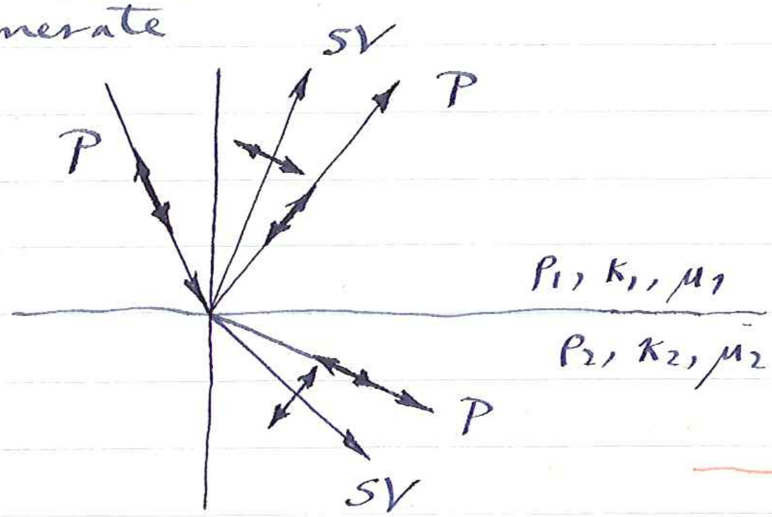

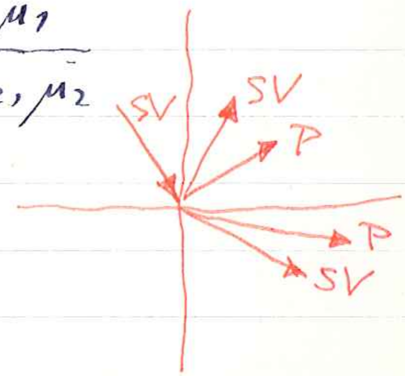

Likewise incident SV can generate P as well as SV. Analysis of this situation to find the <u>amplitudes</u> of the four generated waves is slightly complicated.

Note: SH particle motion is purely <u>horizontal</u>, cannot be detected by vertical motion instrument.

Often in studying S waves investigators limit themselves to SH waves to avoid SV → P conversion problems.

This is easy to do. Consider map view at station

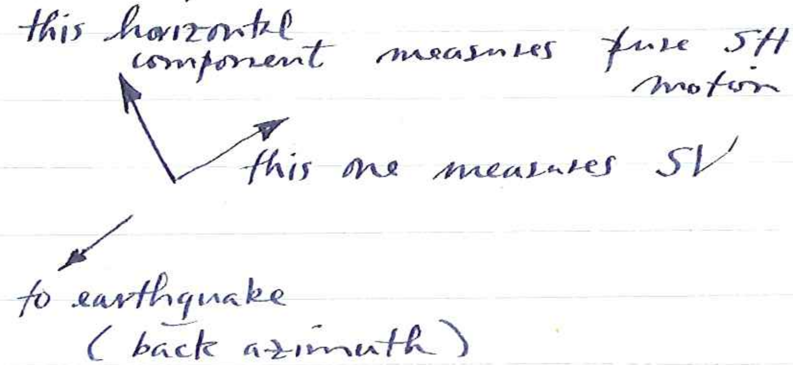

Usually instruments oriented NS and EW. Must be digitized and <u>rotated</u> to separate SH.

We shall find the P-SV and SH separation prevails in other branches of seismology also

body waves	surface waves	modes
SH	Love	toroidal ${}_nT_\ell$
P-SV	Rayleigh	spheroidal ${}_nS_\ell$

To find the <u>amplitudes</u> of reflected and transmitted waves is slightly complicated but we can easily find the ray paths and travel times by an extension of

geometrical optics.

Consider a wave of any type impinging and one of any other type leaving, e.g.

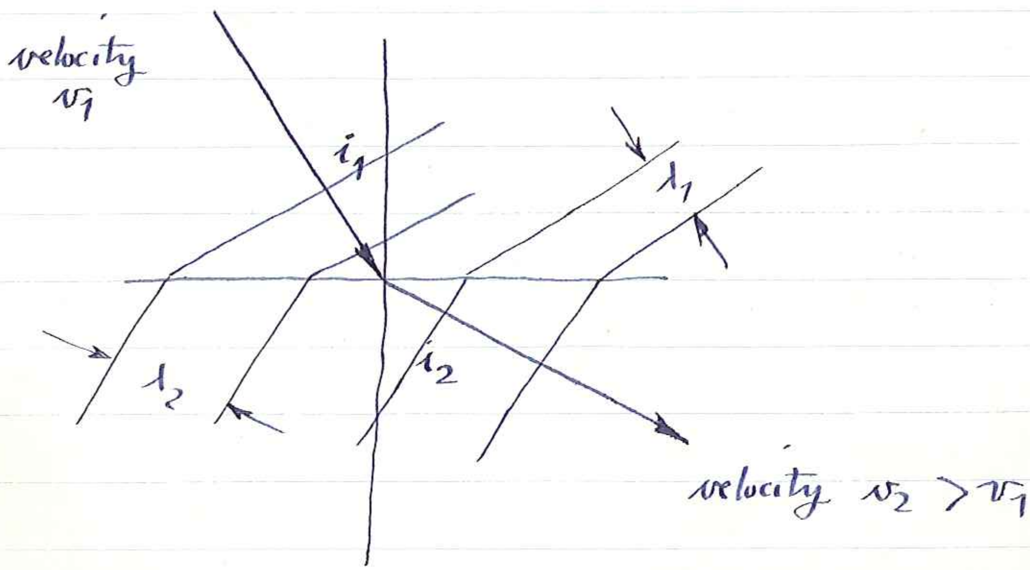

Incoming wave period T, wavelength λ_1, outgoing same period T (can't change), wavelength λ_2

Thus

$$\boxed{T = \frac{\lambda_1}{v_1} = \frac{\lambda_2}{v_2}}$$

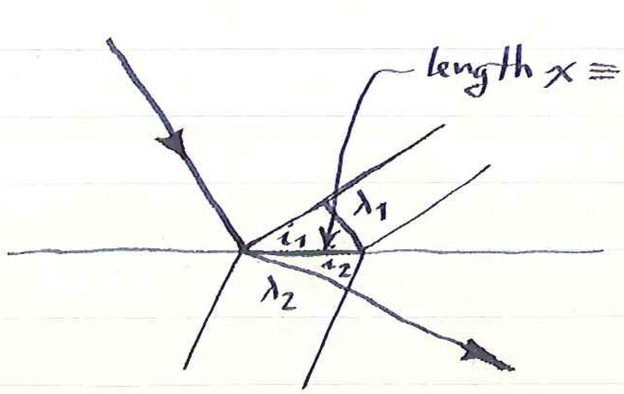

But we also have

$\lambda_1 = x \sin i_1$, $\lambda_2 = x \sin i_2$

Thus $$\boxed{\frac{\sin i_1}{v_1} = \frac{\sin i_2}{v_2}}$$ Snell's law

Governs both reflected and refracted waves, including P–SV conversions, e.g.

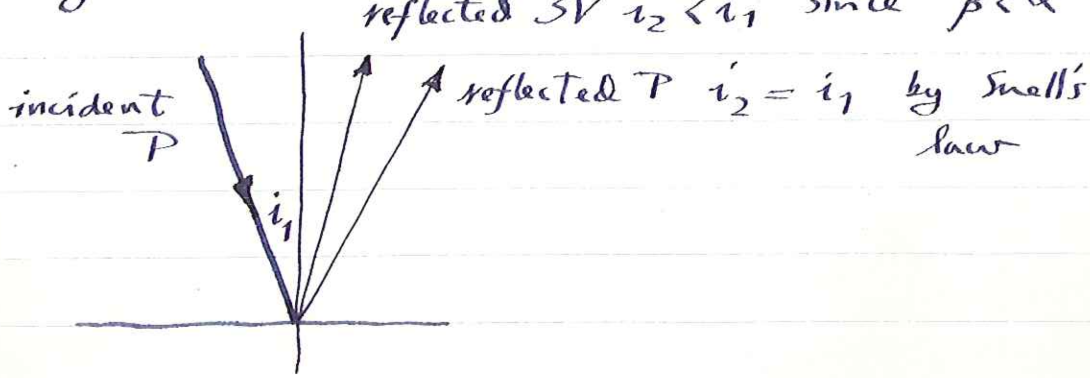

Alternatively Snell's law can be derived from Fermat's principle. Consider the refraction case

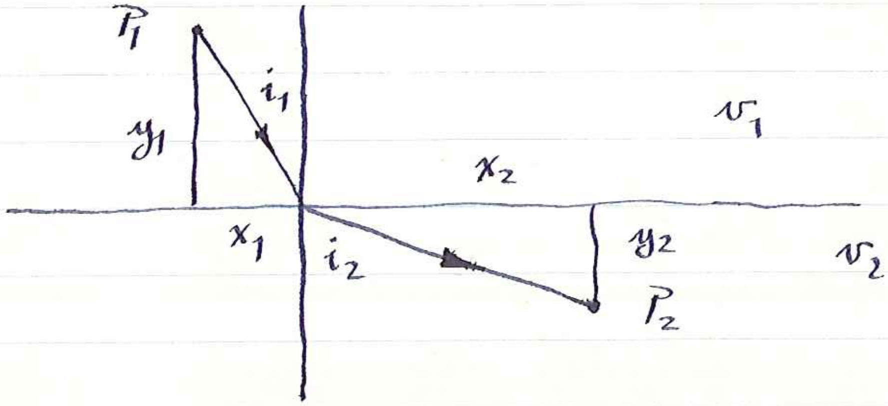

We know in both media 1 and 2 that

ray paths must be <u>straight lines</u>. Consider all possible connected straight line paths between P_1 and P_2.

$$T = \frac{y_1}{v_1 \cos i_1} + \frac{y_2}{v_2 \cos i_2}$$

Also $\quad x_1 + x_2 = C = \text{constant}$, or

$$\star \quad y_1 \tan i_1 + y_2 \tan i_2 = \text{const}$$

y_1 & y_2 are fixed

By Fermats' principle

$$\delta T = \frac{y_1}{v_1} \frac{\sin i_1}{\cos^2 i_1} \delta i_1 + \frac{y_2}{v_2} \frac{\sin i_2}{\cos^2 i_2} \delta i_2 = 0$$

Fermat

But from $\star$

$$\frac{y_1}{\cos^2 i_1} \delta i_1 + \frac{y_2}{\cos^2 i_2} \delta i_2 = 0$$

$$\delta i_1 = - \frac{y_2}{y_1} \frac{\cos^2 i_1}{\cos^2 i_2} \delta i_2$$

$$\delta T = \left[- \frac{y_2}{\cos^2 i_2} \frac{\sin i_1}{v_1} + \frac{y_2}{\cos^2 i_2} \frac{\sin i_2}{v_2} \right] \delta i_2 = 0$$

Must vanish for arbitrary δi_2. Thus

$$\boxed{\frac{\sin i_1}{v_1} = \frac{\sin i_2}{v_2}}$$ Snell's law

If we compute the second variation $\delta^2 T$ we find $\delta^2 T > 0$, T is a minimum time path, the ray goes down to get out of the slower medium 1 more quickly.

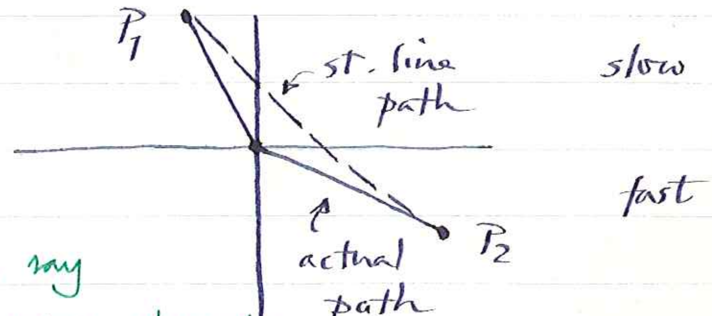

For the same reason ray paths in the mantle curve upwards

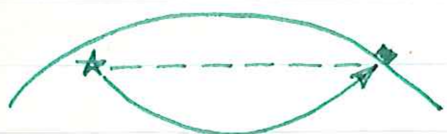

Snell's law enables us to find the ray paths and arrival times of reflected and refracted phases. The laws governing their amplitudes are more complicated, the transmission and reflection coefficients depend on incidence angle and on ρ_1, κ_1, μ_1 and ρ_2, κ_2, μ_2 across the boundary in a rather complicated way.

We shall give but two examples. The simplest case is incident SH.

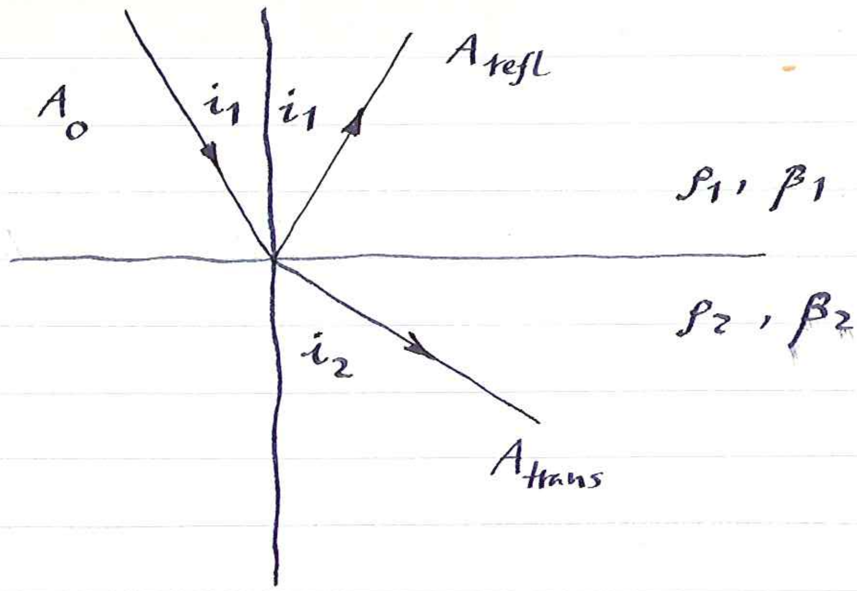

both solid media

incident amplitude A_0, say
Then it can be shown that

$$\boxed{A_{refl} = \frac{\rho_1\beta_1 \cos i_1 - \rho_2\beta_2 \cos i_2}{\rho_1\beta_1 \cos i_1 + \rho_2\beta_2 \cos i_2} A_0}$$

Note → dependence on both ρ and β

$$\boxed{A_{trans} = \frac{2\rho_1\beta_1 \cos i_1}{\rho_1\beta_1 \cos i_1 + \rho_2\beta_2 \cos i_2} A_0}$$

(actually only on product $\rho\beta$, the impedance)

$\boxed{\cancel{A_{refl} + A_{trans} = A_0}}$

The second relatively simple special case is reflection off a free surface.

For SH, can be shown that there is complete reflection with no change of phase for every incident angle

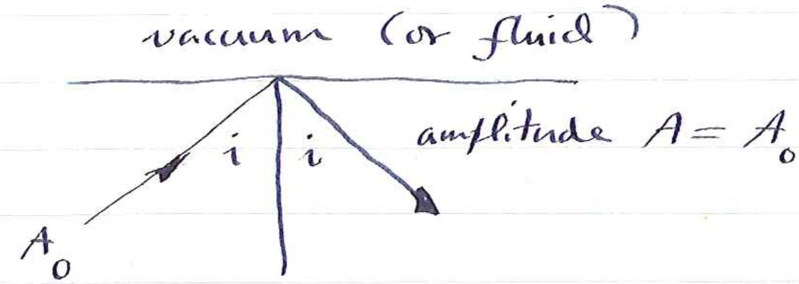

For incident P or SV, get both reflected P and SV, thus $\exists$ 4 possible reflection coefficients

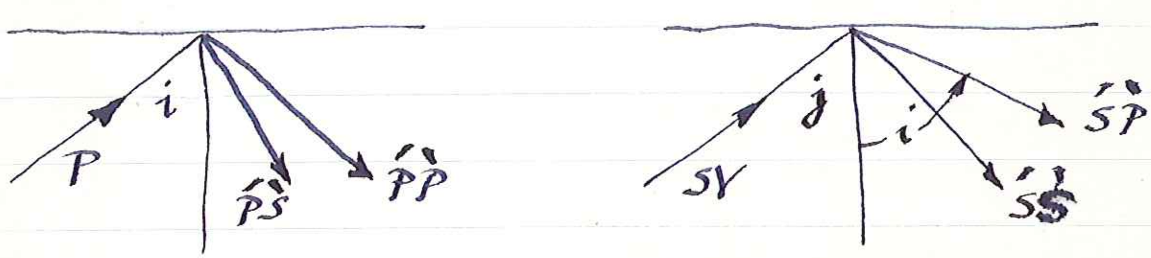

Note notation: i for P waves, j for S waves.

A plot of these four for $i < 90°$ is shown in Aki + Richards Fig. 5.6, plotted against horizontal slowness but there is a distorted angle scale at the top. Note: for incident SV i is the reflected angle of the P wave.

$i = 90^\circ$ is the critical angle for reflected P. For j even greater, all reflected energy is SV and $|\acute{S}\grave{S}| = 1$, see Figure 5.10.

For shallow angles of incidence $i \gtrsim 45^\circ$ or so, the reflected motion is in both cases almost all opposite in type from the incident motion, incident P is converted almost totally to reflected SV and vice-versa.

The plots are for the case $\alpha = 5$ km/s and $\beta = 3$ km/s, typical values for the Φ's const. Beyond the critical angle SV is said to suffer total internal reflection. The $\acute{P}\grave{S}$ amplitude shown is that of the inhomogeneous wave.

The critical angle is given by Snell's law

$$\frac{\sin i}{\alpha} = \frac{\sin j}{\beta}, \quad \sin i = 1 \text{ for } i = 90^\circ$$

$$\boxed{j = \arcsin(\beta/\alpha)}$$

in example shown $\frac{\beta}{\alpha} = \frac{3}{5}$

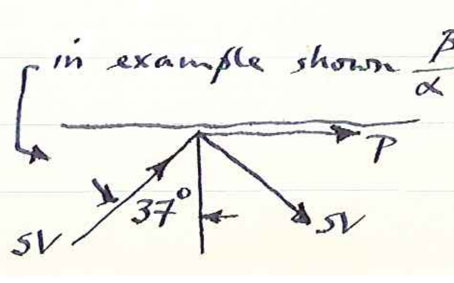

SH is always totally internally reflected and SV is for $j > j_{crit}$.

There is also a critical angle phenomenon in the reflection off a discontinuity between 2 materials, e.g. SH

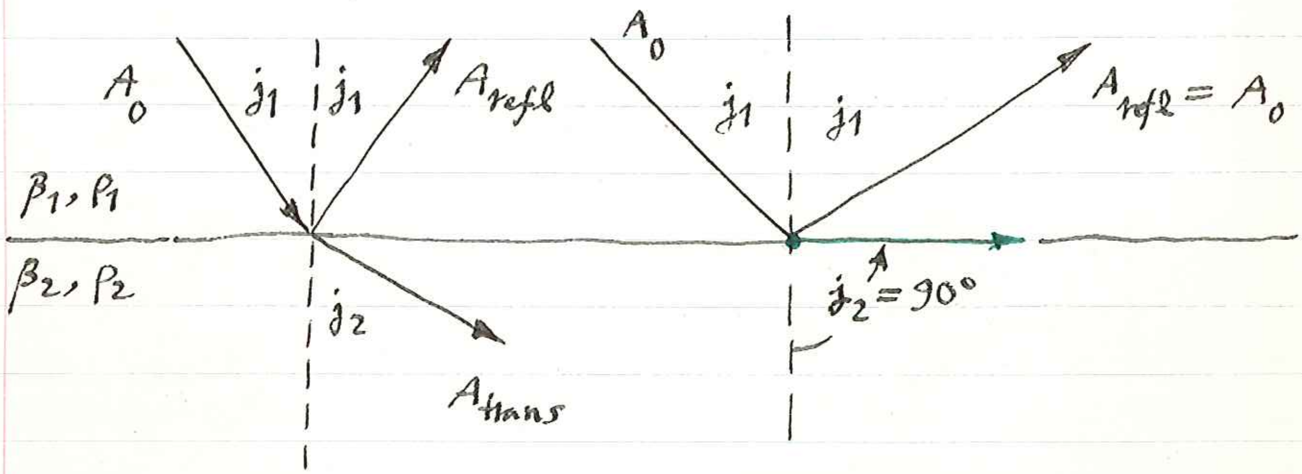

j_1^{crit} occurs when $j_2 = 90°$ or when

$$\boxed{j_1^{crit} = \arcsin \frac{\beta_1}{\beta_2}}$$

Our previous formula for A_{refl} then shows that $A_{refl} = 1$.
Wide-angle reflections beyond the critical angle are totally reflected, thus typically a strong signal at great enough distance

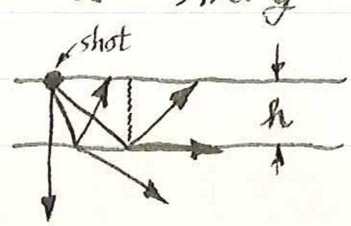

must be a distance $2h \tan i_{crit}$ away to see wide-angle reflections.

In this simple example of reflection from the free surface of a solid half-space, we have now obtained specific formulas for each component of the matrix

$$\begin{pmatrix} \acute{P}\grave{P} & \acute{S}\grave{P} \\ \acute{P}\grave{S} & \acute{S}\grave{S} \end{pmatrix}.$$

This matrix summarizes all possible reflection coefficients, and it is called a *scattering matrix*. Each of its components is plotted against slowness in Figure 5.6, and for this very simple interface, the components are found to vary quite strongly. Only the range $0 \le p \le 1/\alpha$ is shown. For slowness in the range 0.14 to 0.195 sec/km, note that the reflected motion is almost all opposite in type from the incident motion. That is, incident P is converted almost totally to reflected SV, and incident SV to reflected P. Far more complicated behavior can occur in other interface problems (solid/fluid, etc.), and seismologists are often forced to evaluate this behavior in great detail in order to interpret a particular piece of data. For convenience, therefore, we shall give the coefficient

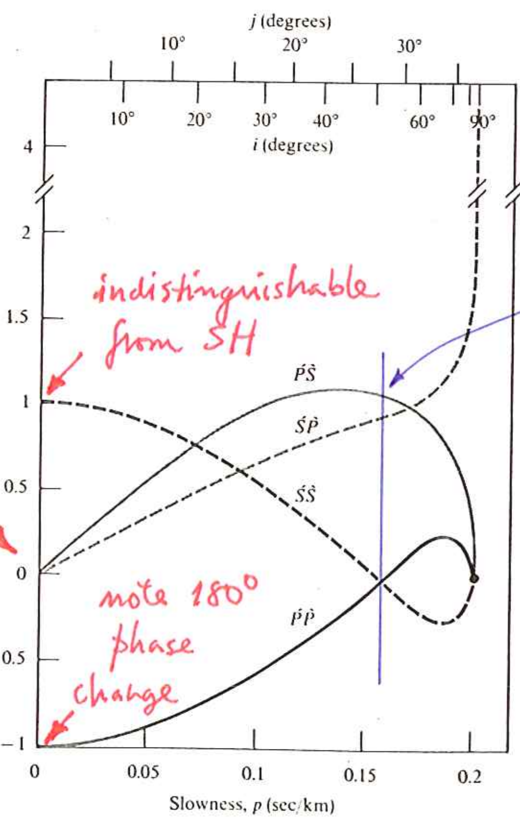

indistinguishable from SH

no P–S conversion at normal incidence

note 180° phase change

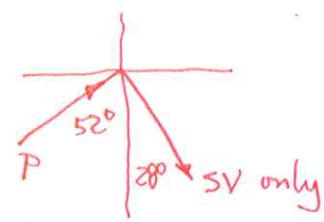

complete P → SV conversion at $i \approx 52°$

FIGURE 5.6

The four possible P-SV reflection coefficients (displacement amplitude ratios) for a free surface are shown against horizontal slowness p. See Figure 5.5. In this case, α = 5 km/sec and β = 3 km/sec, and we restrict p to lie in the range $0 \le p \le 1/\alpha$ so that incidence angle i is always real. For i = 90°, $\acute{S}\grave{P}$ is quite large (~4.1).

ditto

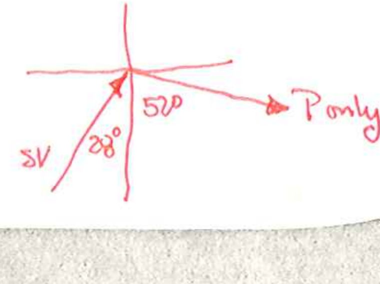

In Figure 5.10, we show $\acute{S}\grave{P}$ and $\acute{S}\grave{S}$ as functions of p in the range $0 \leq p \leq 1/\beta$, giving both amplitude and phase.

As another example of the need for using inhomogeneous waves, consider the reflection and transmission of SH-waves, as described in Figure 5.7 and equations (5.32). Inhomogeneous waves will be present in the upper medium if $1/\beta_1 < p$, and then this wave attenuates away from the interface, provided that we again choose

$$\frac{\cos j_1}{\beta_1} = +i\sqrt{p^2 - \frac{1}{\beta_1^2}} \qquad \text{(in the case } \omega > 0\text{)}, \tag{5.49}$$

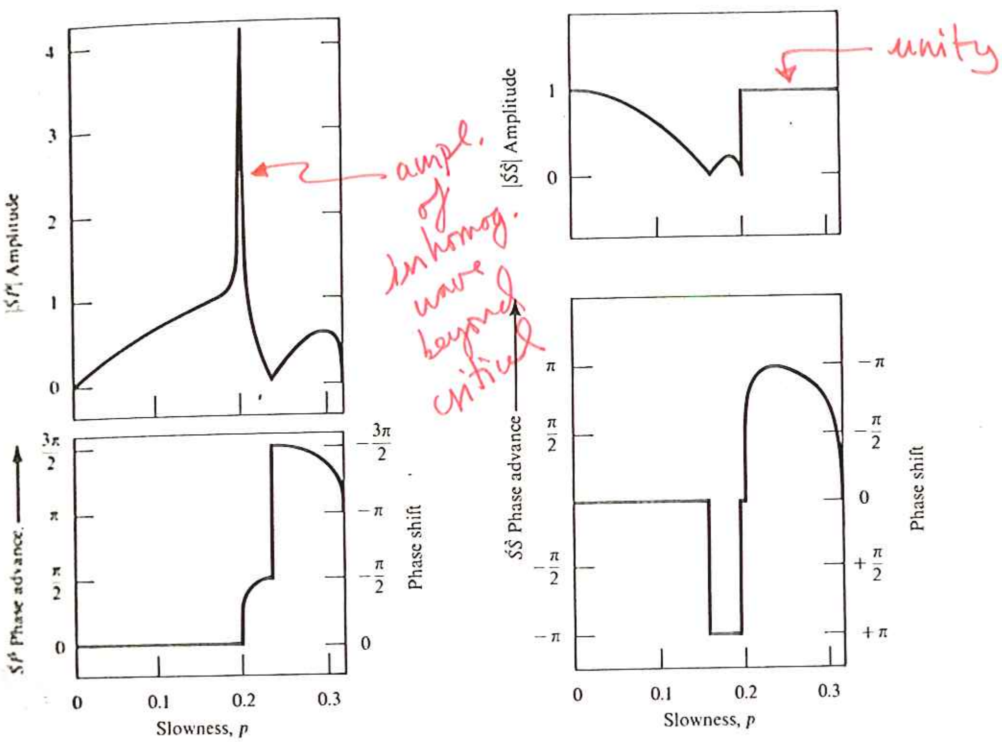

FIGURE 5.10

The amplitude and phase of two reflection coefficients are shown as a function of horizontal slowness p. The coefficients are $\acute{S}\grave{P}$ and $\acute{S}\grave{S}$ for an SV-wave incident on the free surface, and we have taken $\alpha = 5$ km/sec, $\beta = 3$ km/sec, so that these coefficients have already been shown in Figure 5.6 for the range $0 \leq p \leq 1/\alpha$. Here we extend the range to $0 \leq p \leq 1/\beta$, so that an inhomogeneous P-wave is present for the range $1/\alpha < p \leq 1/\beta$. We have chosen to emphasize phase advance rather than phase shift, since the former is a quantity independent of the sign of frequency and independent of our Fourier sign convention. The phases actually plotted are those of $\acute{S}\grave{P}$ and $\acute{S}\grave{S}$ as determined by (5.30) and (5.31). Note that zeros in the coefficients are now associated with jumps of amount π in phase.

Seismic ray theory in spherical Earth

Both $\alpha(r)$ and $\beta(r)$ fcns only of radius.

$$\boxed{\text{An immediate consequence of Fermat: ray paths in this case always lie in planes passing through center of } \oplus.}$$

Problem thus reduced to 2 dimensions.

Why is it useful to speak of P and S rays separately?
Earth has several major discontinuities. Two most important are inner core–outer core and core–mantle. The Moho is a less profound discontinuity than these two, there are also near disconts. or sharp gradient zones near 400 and 650 km depth in mantle.

also $\oplus$'s surface, obviously.

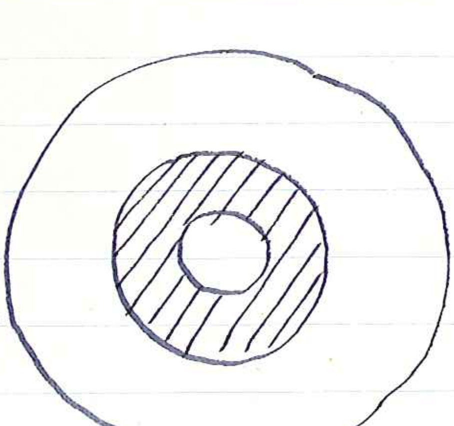

These major disconts. give rise to reflections and converted phases.

Can think of mantle as composed of many layers. Each will give rise to reflections and conversions

Consider problem:

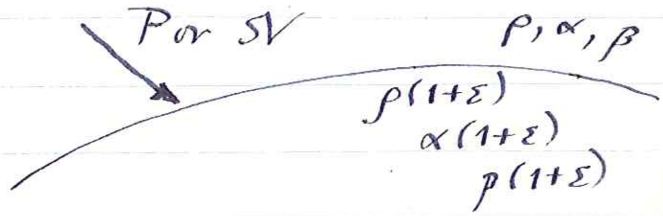

Small contrast in properties, of <u>order</u> $\varepsilon \ll 1$.

Can be shown that if energy of incoming phase is ~~[illegible]~~ E_{inc}, then:

$$\boxed{\begin{aligned} E_{\substack{\text{transmitted as}\\\text{same type}}} &= E_{inc}\left[1 - O(\varepsilon^2)\right] \\ E_{\text{all other types}} &= O(\varepsilon^2) \end{aligned}}$$

This justifies speaking of pure P and pure SV rays in regions without major discontinuities. Energy not transmitted as same type is of <u>second order</u>.

Body wave nomenclature

After a quake energy can arrive at a given station by a variety of stationary time paths. The conventional notation for the various paths is as follows:

- P : P wave in mantle
- S : S wave in mantle
- K : P wave in outer core (no S wave in outer core)
- I : P wave in inner core
- J : S wave in inner core
- c : external reflection off CM boundary
- i : external reflection off IC-OC bdry
- p, s : reflection off free surface

Examples:

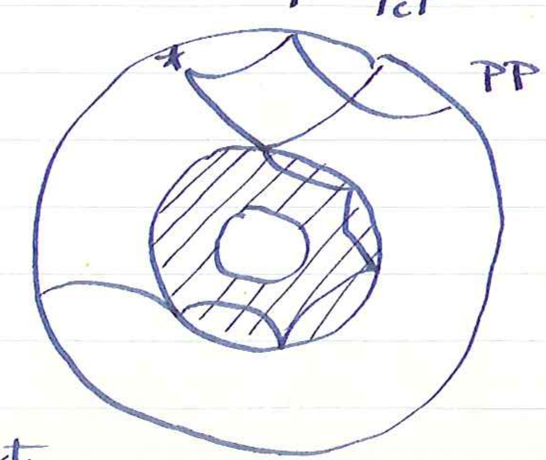

PKKKKP or P4KP for short

Note again: ray paths curve upward throughout most of ⊕ since $\alpha(r)$, $\beta(r)$ decrease with increasing r.

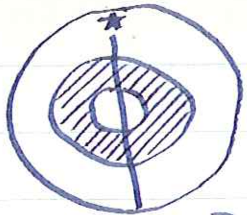

PKIKP straight through ⊕
(T = 22 m for surface
focus quake)

ScS ScSScS or
ScS2 for short

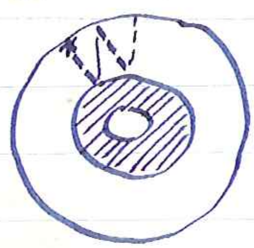

(T = 15.5 m for surface
focus, $\Delta = 0$, ScS)

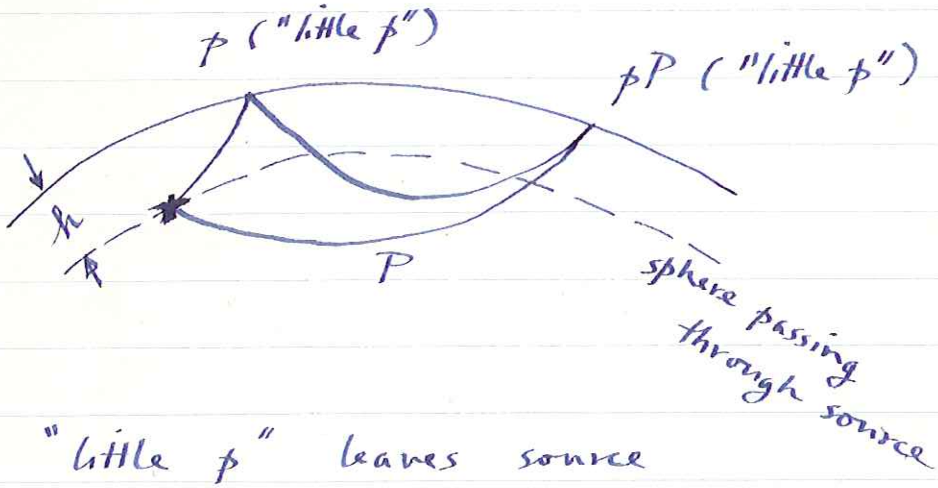

"little p" leaves source
going up rather than down
(out top 1/2 of focal sphere)

Comparing arrival times of pP and P
an excellent way to determine depth
h of a quake, relatively insensitive
to epicentral distance Δ. 1st lab exercise.

Some other notation has been suggested, not in as common a use as above, e.g.

d : reflections off discontinuities in upper mantle

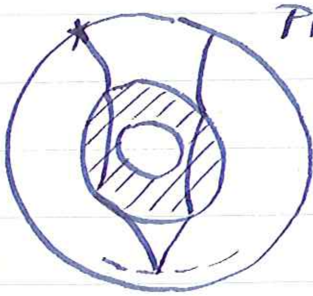

PKPdPKP or P'dP'

$P' \equiv PKP$

also in use : P'400P' for reflection off 400 km discont.

Sp :

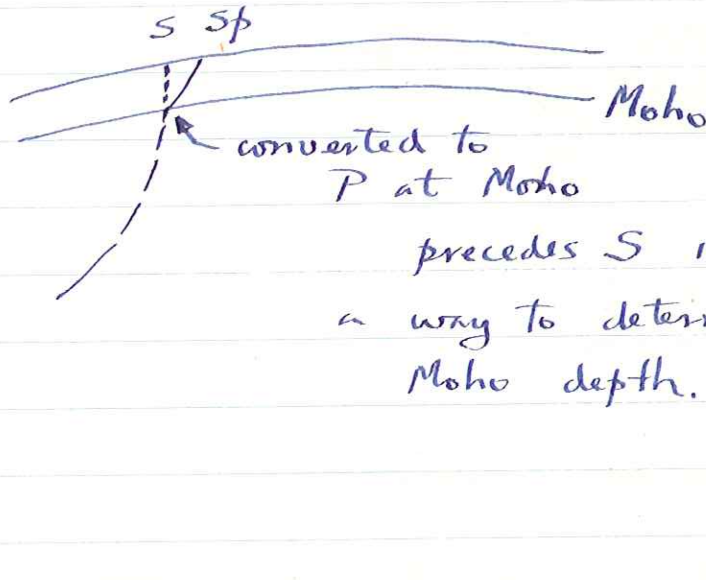

precedes S in time, a way to determine Moho depth.

The ray parameter:

Probably the most important concept in seismology. Consider a ray, P or S, in the $\oplus$:

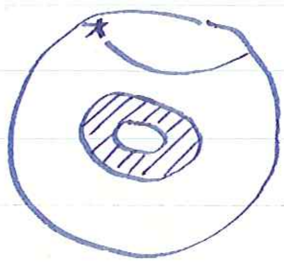

$\alpha(r)$ and $\beta(r)$ are, except for LVZ, increasing fcns of depth, so the rays dive down as shown to arrive along least time paths.

Treat mantle (or core) as limit of ∞ number of very thin concentric layers. Consider two such layers, velocities v, v', radii to base r, r'

← this bdry plays no role in the argument

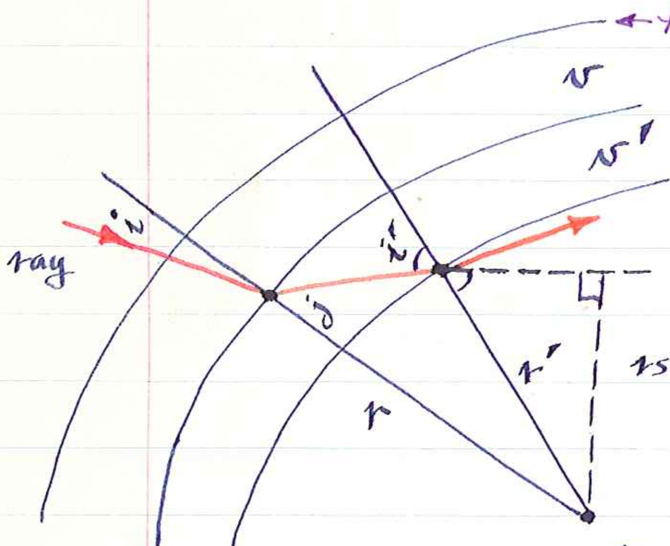

$$r \sin j = r' \sin i'$$

same

Snell's law: $$\frac{r \sin i}{v} = \frac{r \sin j}{v'} = \frac{r' \sin i'}{v'}$$

Thus we see that:

$$\boxed{p = \frac{r \sin i}{v} \quad \text{is } \underline{\text{constant}} \text{ along the ray}}$$

Called the parameter of the ray. The various rays radiating from the source have different ray parameters. For a surface focus quake

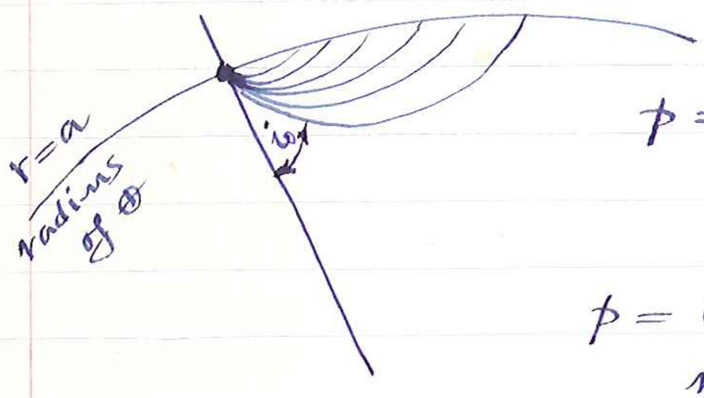

$$p = \frac{a \sin i_0}{v_{crust}}$$

$p = 0$ corresponds to $i = 0$ ray going straight down from source

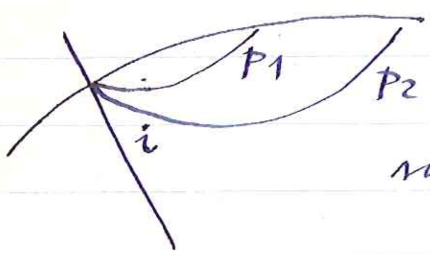

ray parameter $p_2 < p_1$ (actually as we shall soon see this picture is too simple, because of upper mantle triplications.

Units of p (sec per radian).
Conventional to multiply by $\pi/180°$ and

measure in <u>sec / degree</u>, epicentral distances Δ usually measured in <u>degrees</u>. Range of p for P in mantle is 5 – 15 sec / deg.

At <u>bottoming point</u> of ray, radius r_p, $i = 90°$, $\sin i = 1$

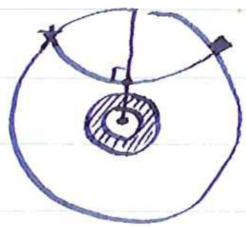

$$\boxed{p = r_p / v(r_p)}$$ *

Note that $1/p$ is simply the <u>angular velocity</u> of the ray or wave

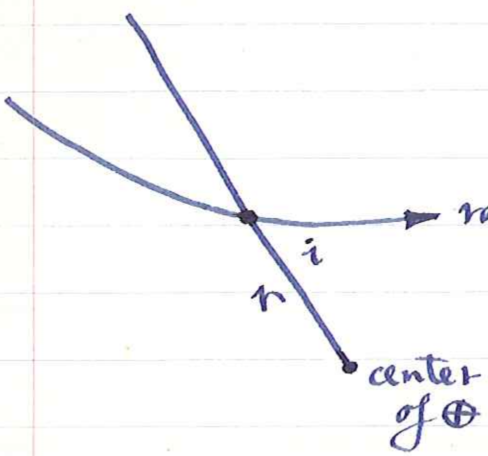

linear velocity of wave at pt. • is

$\underline{v} = \underline{\omega} \times \underline{r}$

$\underline{\omega}$ = angular velocity

But $|\underline{v}| = v$, so $v = \omega r \sin i$, or

$$\boxed{\frac{1}{p} = \frac{v}{r \sin i} = \omega, \text{ angular velocity}}$$

Note from * that if p can be <u>measured</u>, it provides in principle a means of determining v at the bottoming or <u>turning</u> point r_p.

Can p be measured? Yes.

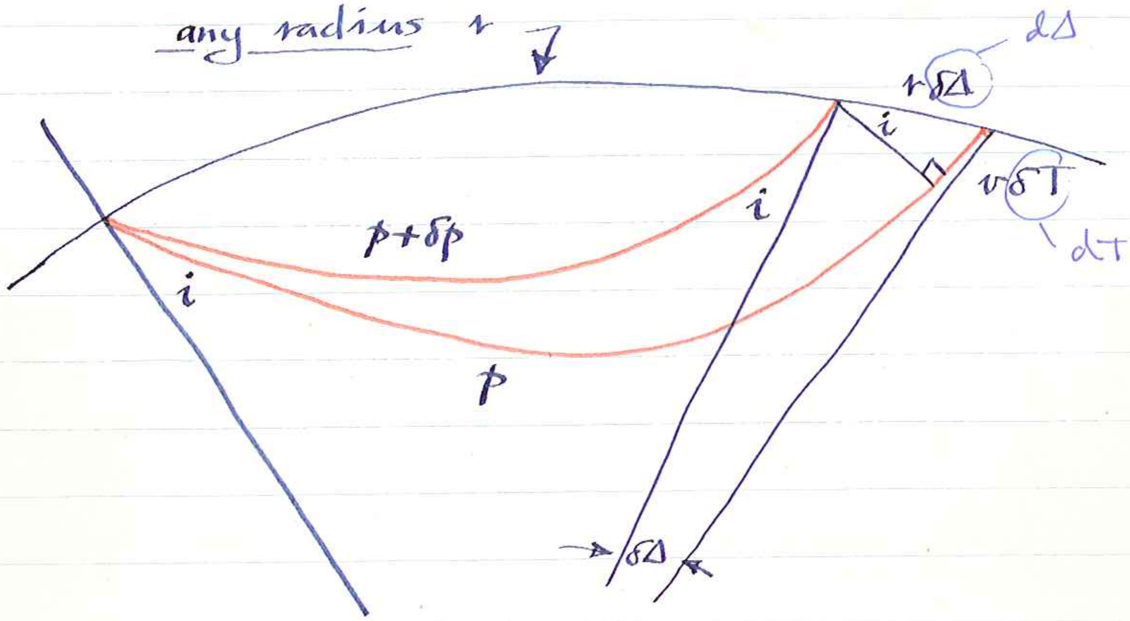

p is the angular slowness

Consider 2 nearby rays p, $p + \delta p$ from <u>same</u> source, at a radius r

Clearly

$$\sin i = \frac{v\,\delta T \;\; dT}{r\,\delta\Delta \;\; d\Delta}, \quad \text{or}$$

$$r \sin i / v = \cancel{\delta T / \delta \Delta} \;\; dT/d\Delta$$

$$\boxed{p = dT/d\Delta}$$

$p(\Delta)$ is the <u>slope</u> of the $T(\Delta)$ <u>travel</u> <u>time curve</u>.

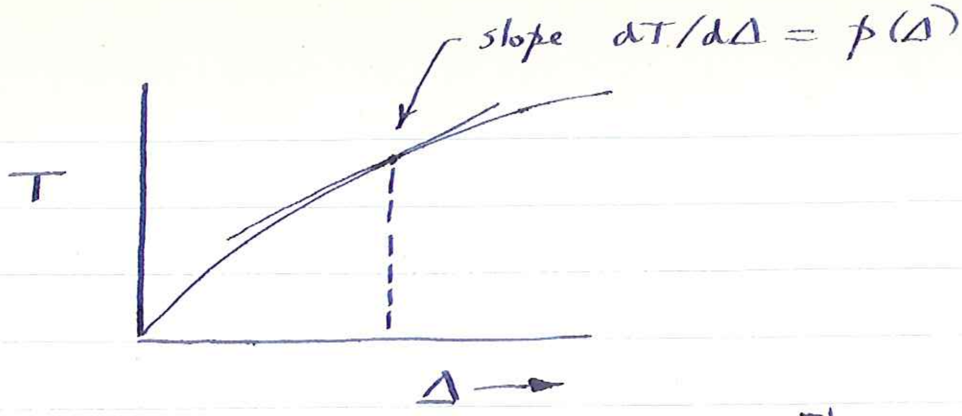

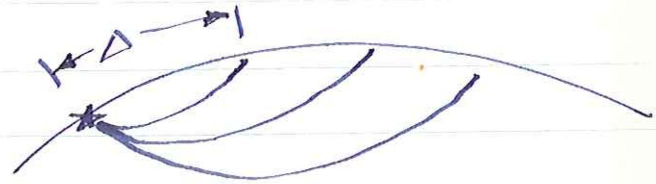

Δ = <u>epicentral</u> <u>distance</u>
(note: epicenter vs. hypocenter)

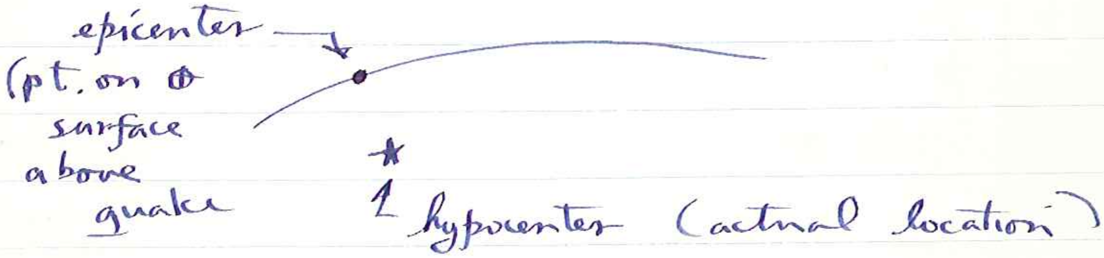

Note: again we have $1/p = d\Delta/dT$, the <u>angular</u> <u>velocity</u> of the ray.

With an <u>array</u> of <u>seismometers</u> p can be measured <u>directly</u>

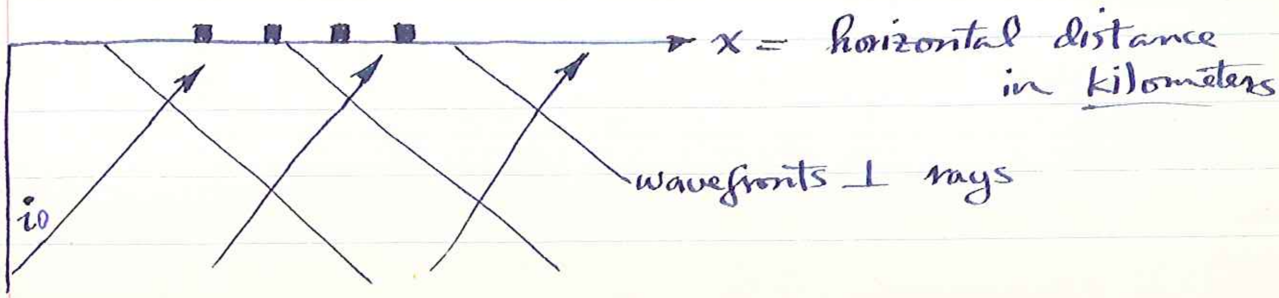

$$p = \frac{a \sin i_0}{v_{crust}} = \frac{dT}{d\Delta} = a\frac{dT}{a\,d\Delta} = a\frac{dT}{dx}$$

$$\boxed{dT/dx = \frac{\sin i_0}{v_{crust}}}$$

dT/dx can be measured directly with an array

$$\boxed{p = a\frac{dT}{dx}}$$

$\frac{dT}{dx}$ = horizontal slowness

dx/dT = apparent velocity of wavefronts as they pass through a horizontal array.

Note the steeper the incoming ray, larger is dx/dT and the smaller is p, $p = 0$ is coming straight up

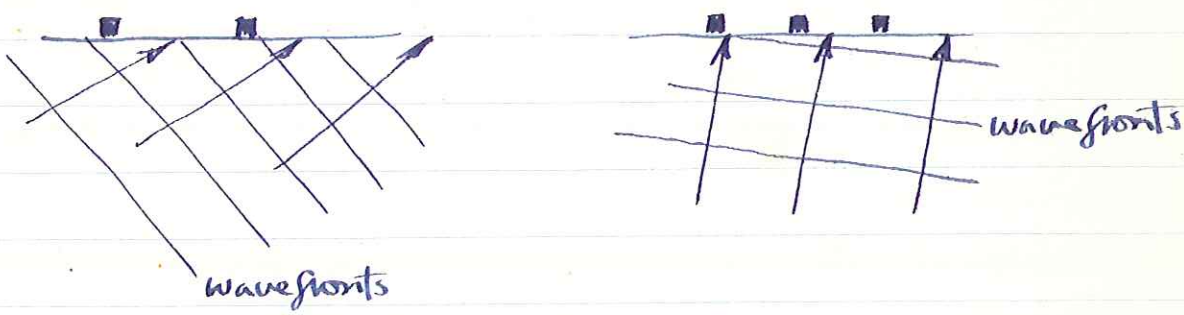

Numerous arrays: LASA, TFSO, NORSAR, S. California, etc.

Alternatively $p(\Delta)$ can be obtained by numerical differentiation of $T(\Delta)$.

Lane Johnson performed a now classical study of $p(\Delta)$ using the TFSO array in Arizona.

Fig. 2 shows location of array, and quakes $\Delta > 30°$ used in study.

Fig. 3 shows <u>measured</u> $p(\Delta)$, smoothly decreasing from about 9 sec/deg at $\Delta = 30°$ to about 4.5 sec/deg at about $\Delta \approx 100°$, near core shadow.

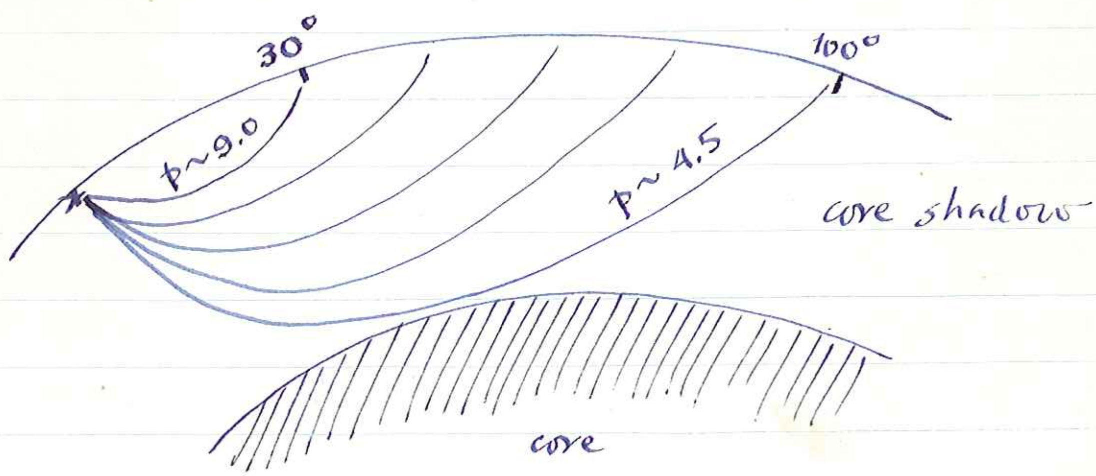

The <u>smooth</u> variation of $p(\Delta)$ for $\Delta > 30°$ indicative of smooth velocity profile below ~ 650 km depth, α increases <u>smoothly</u> from ~ 11 to ~ 13.5 km/sec.

Fig. 9 shows α vs. depth below ~ 650 km depth, with bottoming depths of rays indicated, i.e. ray emerging at 70° from surface source bottoms at about 2000 km depth.

Behaviour of $p(\Delta)$ for $\Delta < 30°$ in contrast very complicated, multiple-valued, see Fig. 4, this due to steep gradients of α vs. r, <u>phase transitions</u> in upper mantle.

Fig. 5 shows location of array in more detail.

The forward problem of body wave seismology:

Given an ⊕ model $v(r)$ how do we find $T(\Delta)$ or $p(\Delta)$?
This problem is easy.

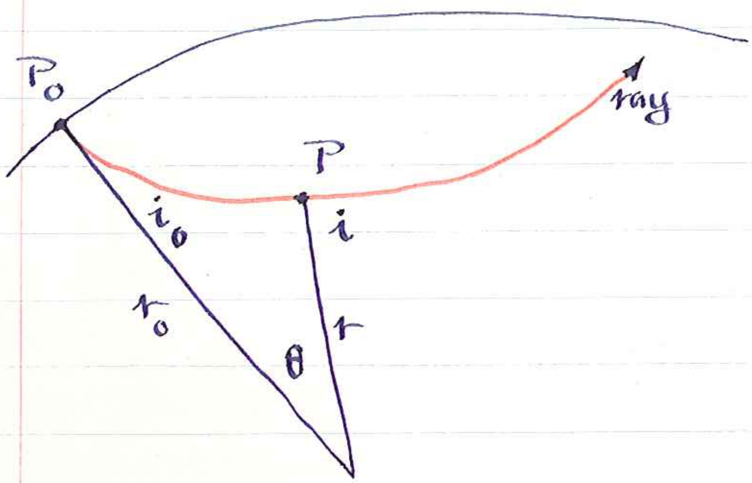

i_0: initial incidence ∠
i: incidence ∠ at pt. P (arbitrary pt. on ray)
r, θ : polar coords

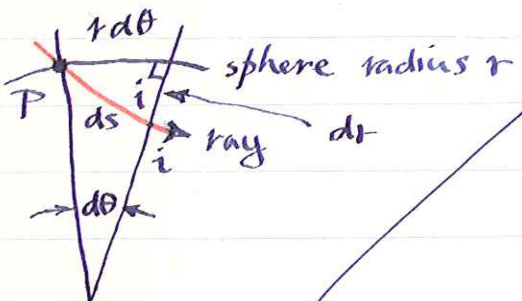

$$\sin i = \frac{r\,d\theta}{ds}$$

ds = an incremental distance along ray

$$ds = \frac{r}{\sin i}\,d\theta = \frac{r^2}{vp}\,d\theta$$

$$ds^2 = dr^2 + r^2\,d\theta^2$$

two equations

$$\boxed{\begin{aligned} ds &= \frac{r^2}{vp}\,d\theta \\ ds^2 &= dr^2 + r^2\,d\theta^2 \end{aligned}}$$

eliminate dθ from these two.

$$\frac{p^2v^2}{r^2} = r^2\left(\frac{d\theta}{ds}\right)^2 = 1-\left(\frac{dr}{ds}\right)^2$$

$$\left(\frac{dr}{ds}\right)^2 = 1-\frac{p^2v^2}{r^2}$$

We shall need $r/v(r)$ a lot. Call it:

$$\boxed{\eta(r) \equiv r/v(r)}$$ – a fn. only of radius.

$$\left(\frac{dr}{ds}\right)^2 = \frac{\eta^2-p^2}{\eta^2} \qquad \left(\frac{ds}{dr}\right)^2 = \frac{\eta^2}{\eta^2-p^2}$$

$$ds = \pm\,\eta\,(\eta^2-p^2)^{-1/2}\,dr$$

The time to travel ds is

$$dT = \frac{ds}{v} = \pm\,\frac{\eta^2}{r}\,(\eta^2-p^2)^{-1/2}\,dr$$

sign depends on whether wave is travelling up ($dr>0$) or down ($dr<0$)

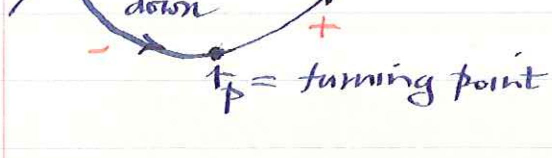

$\eta = \frac{r}{v}$ always $> p = \frac{r}{v}\sin i$

$+$: wave going up

$-$: wave going down

<u>Total</u> <u>travel time</u>: integrate segments, i.e.

$$T = \int_{\text{ray}} dT = \int \frac{\eta^2 \, dr}{r(\eta^2 - p^2)^{1/2}}$$

What are the limits? <u>Upper limit</u> clearly radius of source or receiver.

<u>Lower limit</u>: two cases.

1. ray <u>reflected</u> off an interface, e.g. PcP

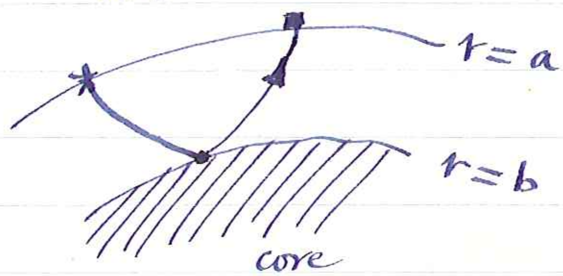

time to travel <u>from r = b to r = a</u> is

$$T = \int_b^a \frac{\eta^2 \, dr}{r(\eta^2 - p^2)^{1/2}}$$

<u>Note</u>: PcP time is twice this (down and back)

2. direct P is <u>not</u> reflected, merely turned around.

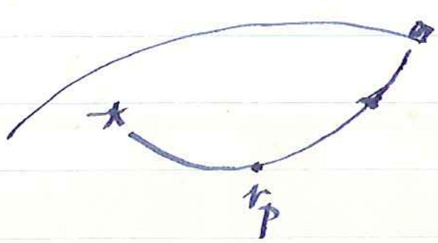

at turning point

$i = 90°$

$p = \eta(r_p)$,

wave is travelling <u>horizontally</u>.

Suppose source at surface $r = a$ as well as receiver, simplest case, then both ray segments are the same.

$$\boxed{T = 2\int_{r_p}^{a} \frac{\eta^2\, dr}{r(\eta^2 - p^2)^{1/2}}}$$

surface focus quake, travel time for ray of parameter p.

We found T by eliminating $d\theta$ from 2 eqns. Let's eliminate ds instead. Find:

$$d\theta = \pm \frac{p}{r}(\eta^2 - p^2)^{-1/2}\, dr$$

$+$: wave going up

$-$: wave going down

$$ds^2 - r^2 d\theta^2 = dr^2$$
$$r^2\left(\frac{\eta^2}{p^2} - 1\right) d\theta^2 = dr^2$$
$$r^2(\eta^2 - p^2)\, d\theta^2 = p^2 dr^2$$

We can use this to find Δ, since

$$\Delta = \int_{\text{ray}} d\theta$$

Thus for the surface focus case:

$$\boxed{\Delta = 2\int_{r_p}^{a} \frac{p\, dr}{r(\eta^2 - p^2)^{1/2}}}$$

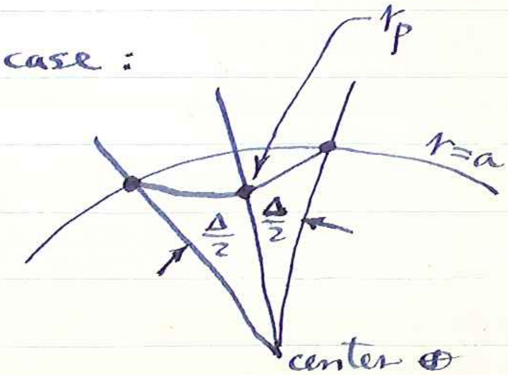

If focus not at surface, must write integral for each segment separately, must do the same for refracted phases such as PKP.

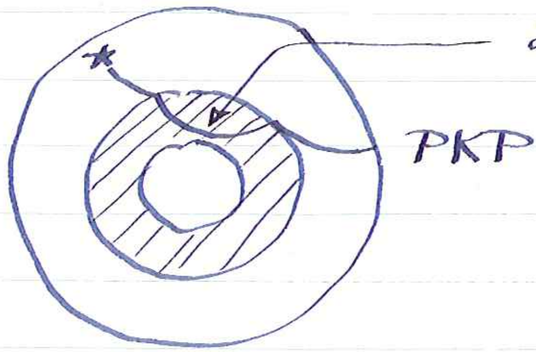

all three segments have <u>same ray parameter</u> p, even if there are strong refractions, reflections or conversions.

This solves the <u>direct</u> or <u>forward problem</u>: given an $\oplus$ model $v(r)$, we can calculate $T(p)$ and $\Delta(p)$, thus $T(\Delta)$ and/or $p(\Delta)$

these the theoretical data or observed quantities for a given model.

<u>Inverse problem</u>: given observations of $T(\Delta)$ or $p(\Delta)$, find $v(r)$ or $\eta(r)$.

Before considering the inverse problem we must pause to consider the complications which may arise in $T(\Delta)$ and $p(\Delta)$ curves.

<u>First</u>, the most important features caused by the <u>fluid core</u>.

The P velocity <u>decreases</u> from ~ 13.7 km/s to ~ 8 km/s at core-mantle bdry

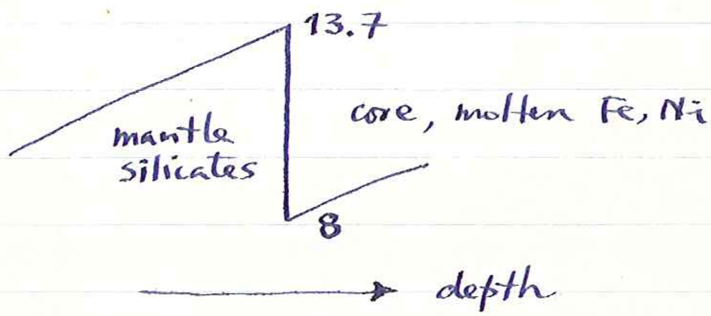

<u>Main</u> reason : fluid $\mu \to 0$, $\alpha = \left(\frac{K + \frac{4}{3}\mu}{\rho}\right)^{1/2}$

not only reason, also major compositional difference.

$\alpha_{core} < \alpha_{mantle}$

$\alpha_{core} > \beta_{mantle}$, but $\approx \beta_{mantle} = 7.2$ km/s

Consider simplest <u>example</u> : <u>homogeneous</u> core and mantle, e.g.

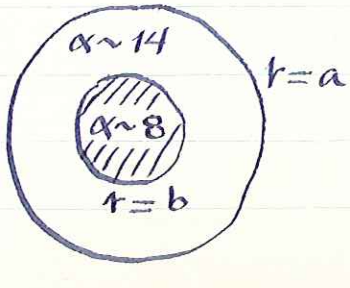

Surface focus quake: consider first P and PcP.

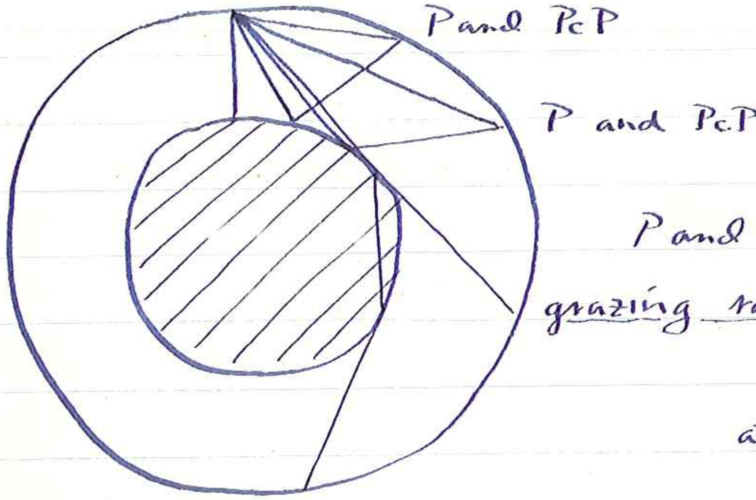

P and PcP merge into one grazing ray, edge of core shadow at $\Delta \sim 105°$ for ⊕'s core.

refracted ray at grazing incidence, emerges at $\Delta \lesssim 180°$ for ⊕

$T \sim 14$ min for ⊕

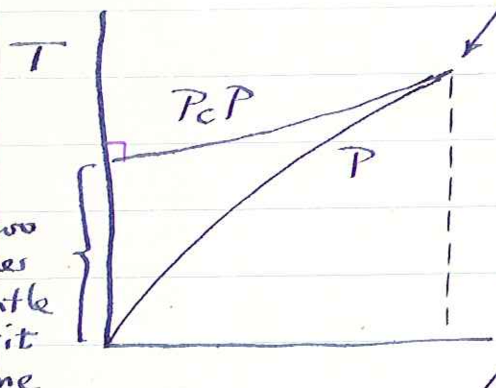

core shadow $\Delta \sim 105°$.

two times mantle transit time (total ~ 8.5 m for ⊕)

$\frac{a}{\alpha}$ (since $i = \frac{\pi}{2}$ at surface)

sharp point at junction

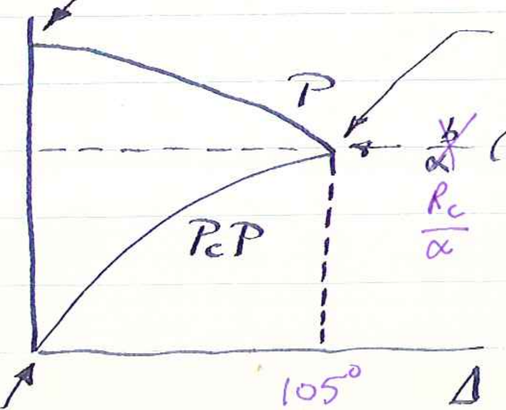

$dT/d\Delta$ decreases for P, increases from 0 for PcP $\quad p = \frac{dT}{d\Delta}$

$\cancel{\frac{b}{\alpha}}$ $\frac{R_c}{\alpha}$ (since $i = \pi/2$ at core)

p of grazing ray for ⊕ is 4.45 sec/degree

$\frac{dT}{d\Delta} = 0$, waves are coming straight up

For Δ beyond the core shadow: PKP waves refracted at core bdry.

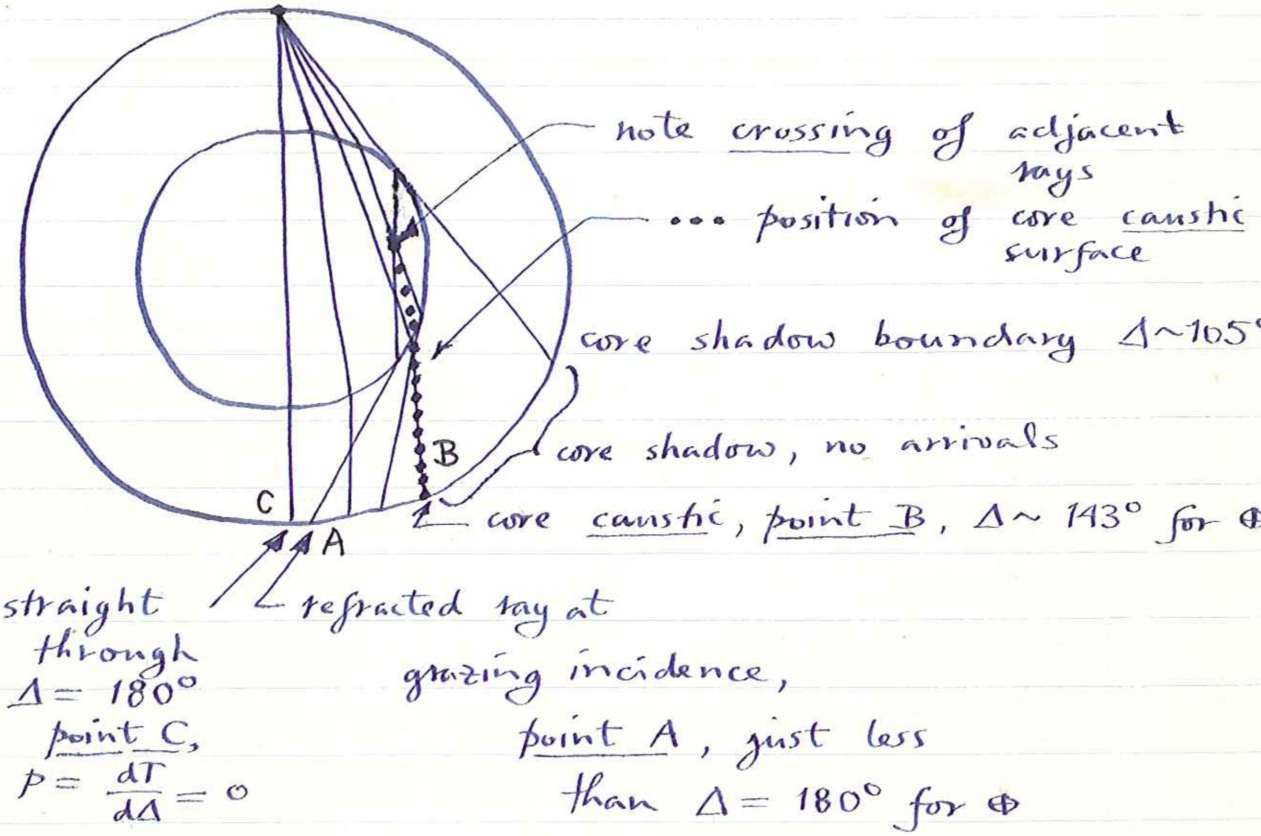

The locus of crossing points of adjacent rays is called the core caustic surface. It can be visualized better in Fig. 9 from Julian + Anderson, shows P, PKP ray paths for a realistic ⊕ model. I've dotted the crossing pts. of adjacent rays.

The $T(\Delta)$ and $p(\Delta)$ curves for the PKP waves have two branches in this simple model PKP_1 and PKP_2.

[redacted]

this as well as A is a sharp pt. since P and PcP have same ray parameter p.

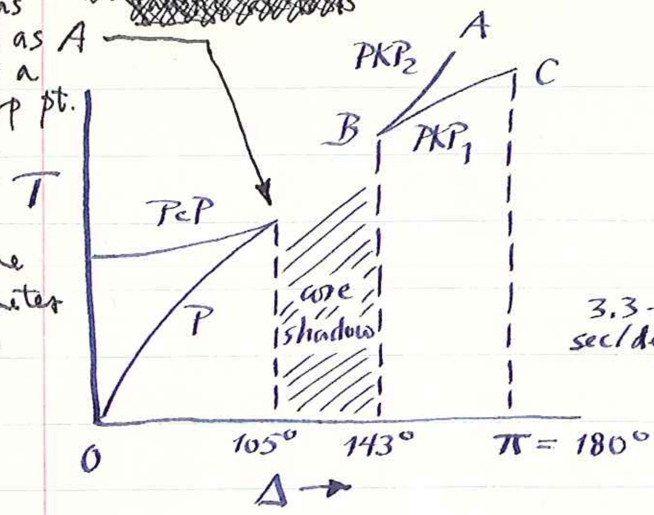

note grazing P and PKP$_2$ at A have same p, $\frac{b}{\alpha} \sim 4.45$ sec/deg

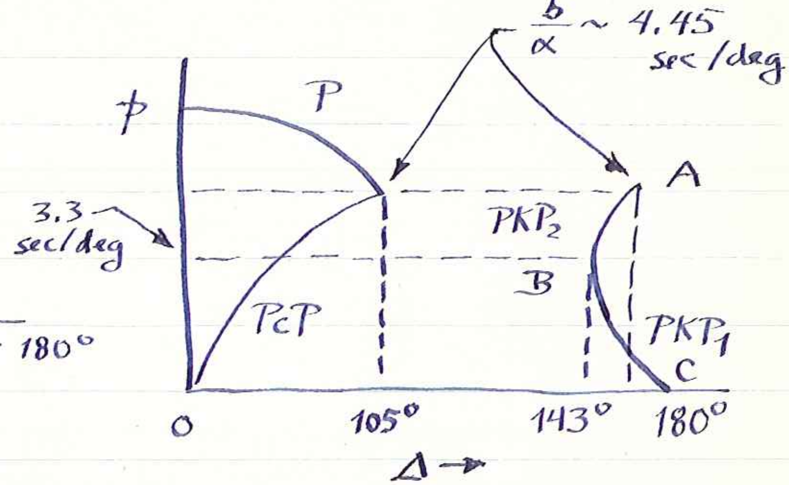

Note: for PKP$_2$ both dT and $d\Delta$ are negative, so $p = dT/d\Delta$ is still positive.

<u>Caustics</u> are recognizable by two features:

1. neighboring rays cross (actually become tangent, the caustic surface is the <u>envelope</u> of all possible rays)
2. $p(\Delta)$ turns <u>vertical</u>, not sharp point as at junction of P and PcP.

Geometrical ray theory, in its simplest form as described here, fails to adequately describe signal at shadow bdry, the caustic point B and points A and C (the antipode). <u>Diffraction</u> effects become important in vicinity of all these pts, e.g. the shadow bdry is <u>not sharp</u>.

PKP in actual Earth:

Oldham (1906): first evidence for low velocity core, observations of P, PcP, P_{diff} near the shadow. $T(\Delta)$ curve thus thought for many years to look like

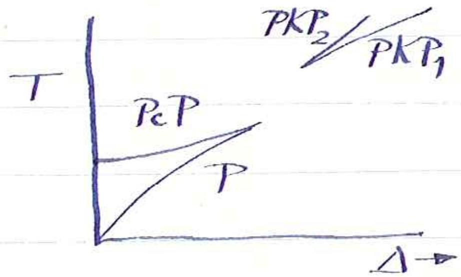

1936 Inge Lehman observed arrivals between 110° and 140° which could not be explained on this basis (they would be in the core shadow). Interpreted as refractions from a high velocity inner core, also reflections from this bdry, Lehman the discoverer of the inner core.
Travel time curve now known to look like:

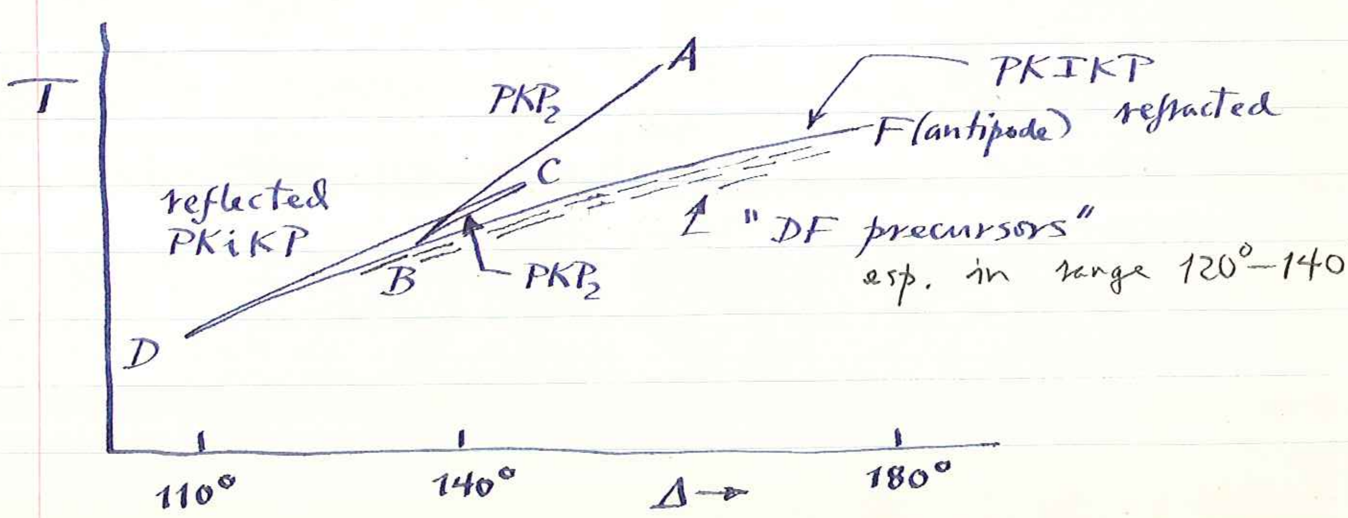

core – mantle bdry. Above T(Δ) curve now thought to be quite reasonable for spherically averaged structure. The velocity structure is quite smooth at IC – OC transition, jumps from about 10 to about 11 km/s, much as envisaged by Ms. Lehman.

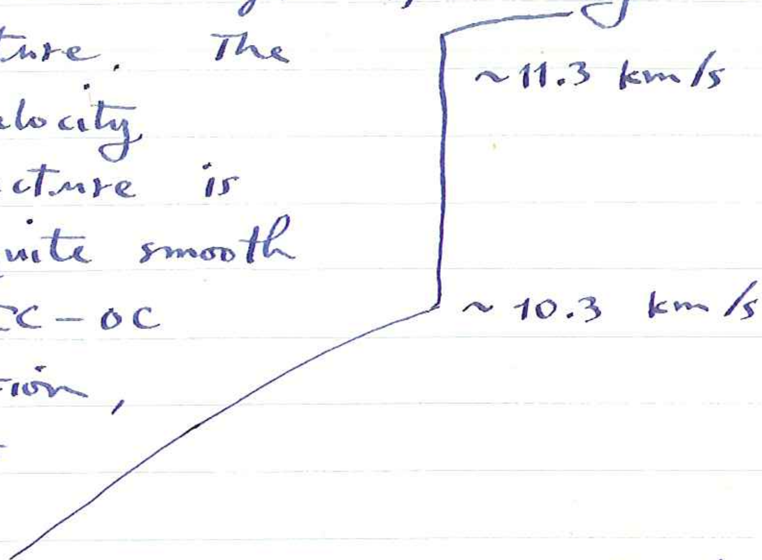

In contrast, core – mantle bdry, current picture: highly inhomogeneous above bdry

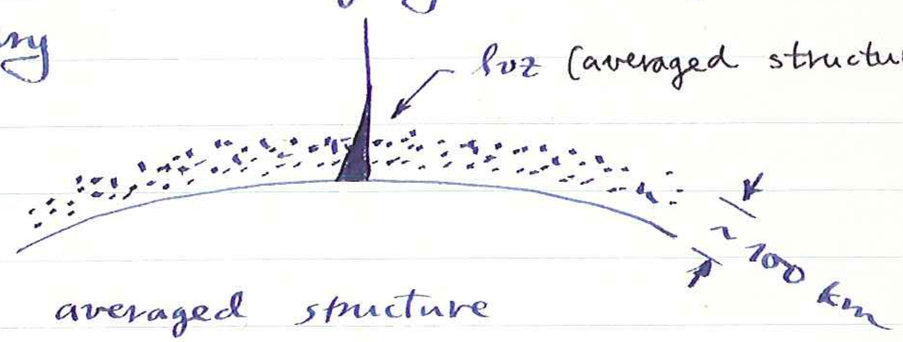

averaged structure seems to have a weak lvz, see e.g. model 1066A

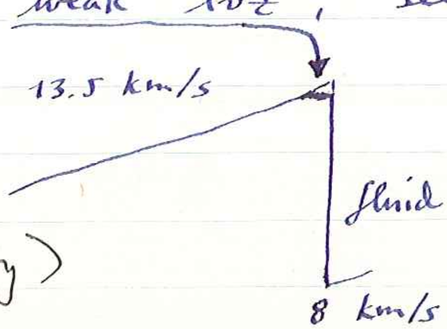

Also suggestion ∃ a Thorne layer (discontinuity)

Current interpretation, thermal bdry layer above core mantle bdry.

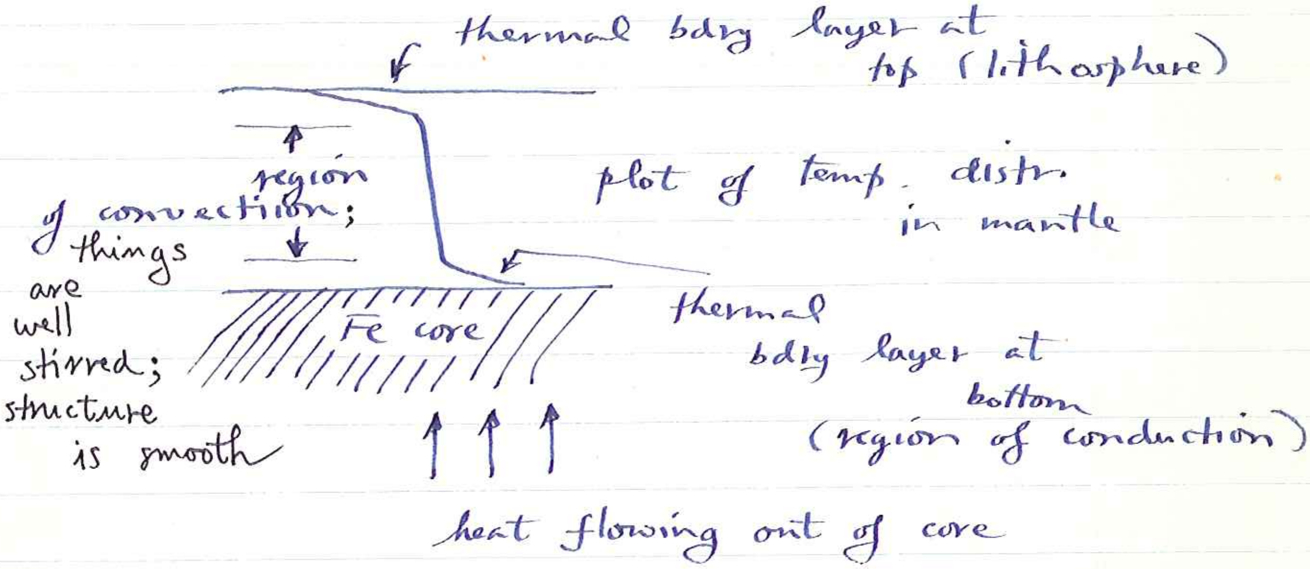

Underside of core-mantle bdry appears on other hand to be very smooth because travel times of P4KP, P7KP, P9KP, P11KP (!) etc. show no increasing scatter, arrivals are sharp and impulsive, see example of P4KP cover of EOS. Any bumps on inside of core must be small ≤ 1 km, whether this large enough to perturb dynamo is debated.

no min. marks ⇒ whole → length shown is less than a minute; this is a short-period record unlike those in our lab.

PnKP rays really get thrown around, see e.g. P7KKP from Chapman, narrow solid angle at source gets sprayed out over 3/4 ⊕ surface ⇒ amplitude small.

Inner core long thought to be solid since this an easy way to ↗ $\alpha(r)$.

Not until 1972 that a claim was made for observation of PKJKP (Julian, Sheppard, Davies) which would be direct proof of solidity.

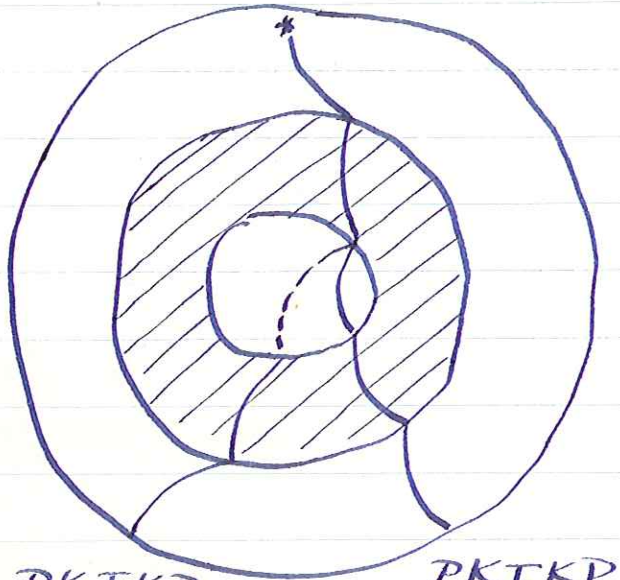

Look for in range $\Delta \sim 230^\circ - 290^\circ$ $T \sim 1/2$ hr. They found a phase in ~ right place.

∃ a major unresolved problem with interpretation. They find $\beta \sim 3$ km/s, cannot be reconciled with $\beta \sim 3.5$ km/s from inversion of free oscillations. Has been suggested they may have seen SKJKP, but they checked dT/dh using quakes of different depths. Its a puzzle.

How are weak body phases looked for in general? Two tricks.

1. use deep focus quakes, not obscured by larger surface waves, we do this in our lab.
2. use beam steering of arrays

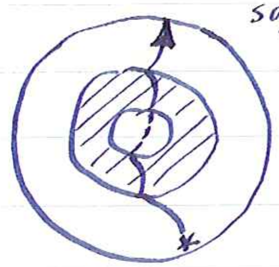

say want to look for a phase with a certain ray parameter p

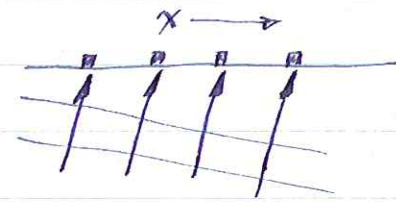

$$p = a\,\frac{dT}{dx}$$

beam steering: simple delay and sum of signals at various seismometers.

Two additional comments:

1. PcP is generally quite a weak signal since reflection coefficient at CM bdry is small (~ 0.1) other 90% is transmitted to become PKP. See Fig. 12 from Buchbinder, disregard data, theoretical value from known contrast in properties, at near vertical incidence almost zero, we look for PcP in lab, can recognize by moveout at several stations, different Δ.

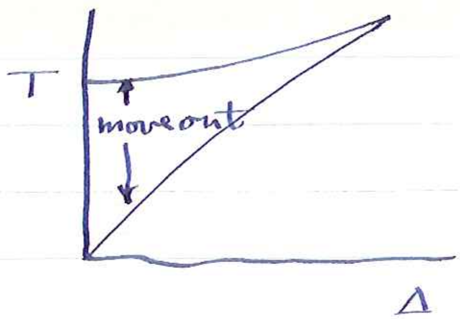

2. Note PKP does not bottom in upper part of core

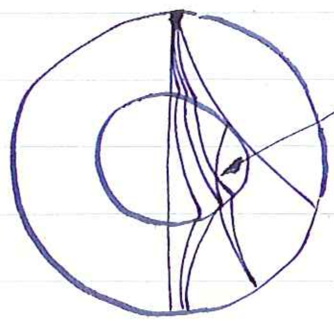

A ray is most sensitive to velocity near bottoming point. This makes it very difficult to use PKP times to find $\alpha(r)$ in outer half of core. We shall see that SKS does not have this problem, and can be (and is) so used. Instead it has a different problem: SKKKS, etc. all come in at ~ same time.

The conclusions regarding S rays in the mantle are similar, get S and ScS merging at core shadow, but $(ScS)_{SH}$ can be a strong arrival since its reflection coefficient is necessarily 1 (∃ no transmitted SH)

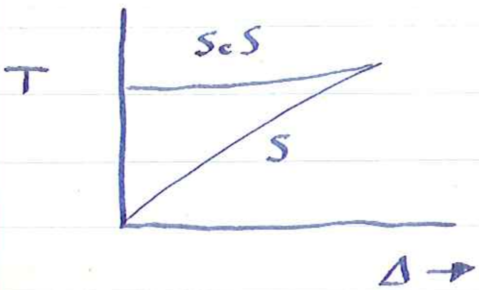

The refracted core waves have quite a different behavior since

$$\beta_{mantle} \sim 7.2 \text{ km/s}$$
$$\alpha_{core} \sim 8.0 \text{ km/s}$$

$$\boxed{\beta_{mantle} < \alpha_{core}}$$

discuss critical angle in more detail

PKP core rays existed for all incident angles, but now there is a critical angle i_c beyond which no rays are refracted into the core.

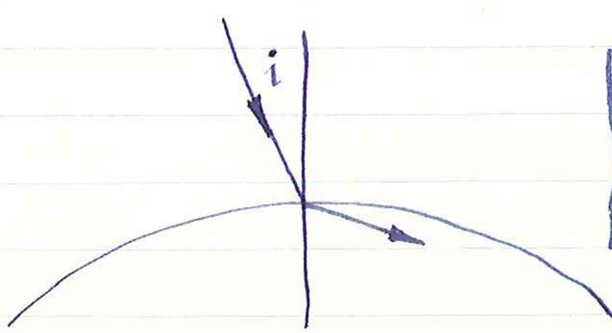

$$\boxed{\begin{array}{l} i_{refr} = 90° \\ \sin i_c = \beta_{mantle} / \alpha_{core} \end{array}}$$

Consider possible SKS rays, starting from 180°:

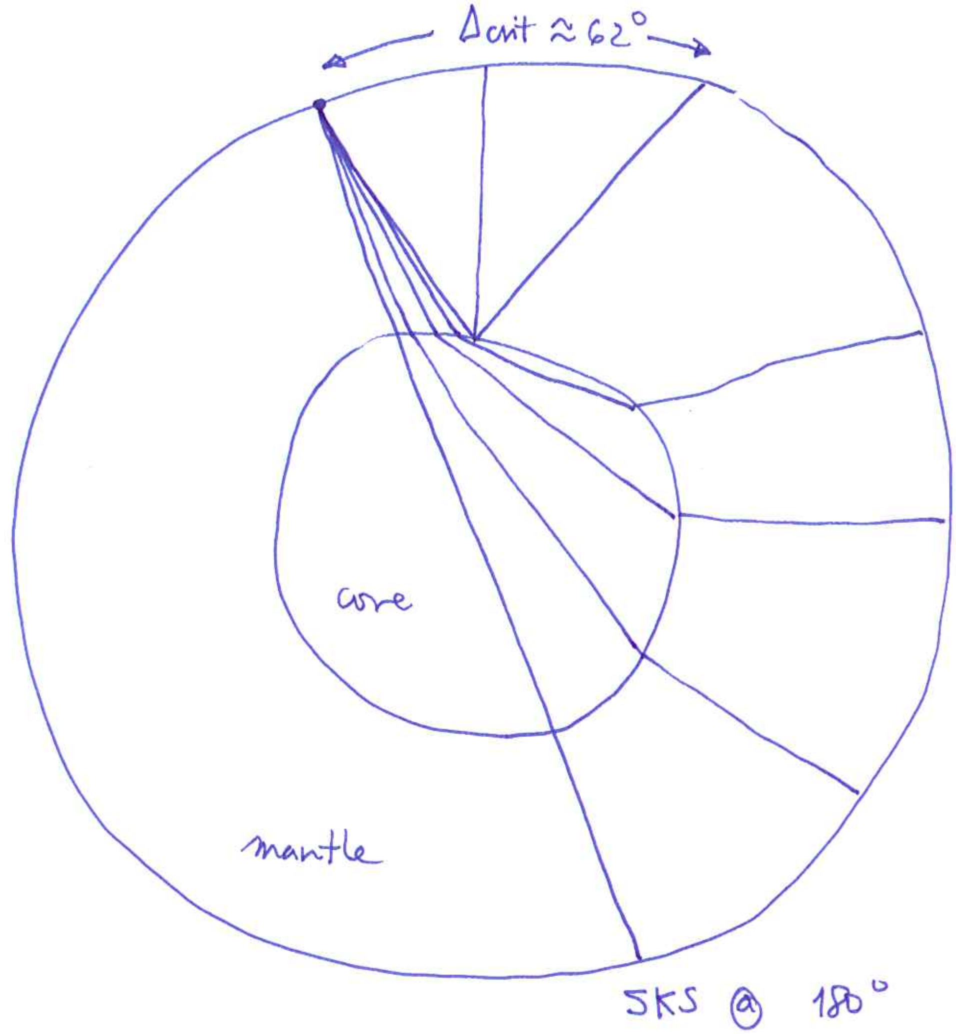

SKKS @ $\Delta = 360°$

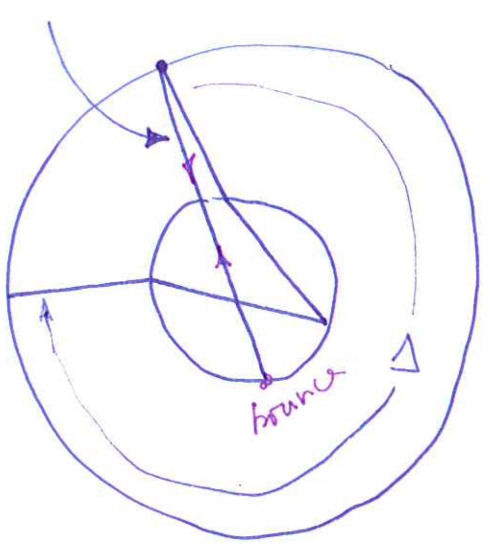

SKKS at angles > 180° look like this

Thus we have, for the <u>homogeneous</u> core and mantle case considered before,

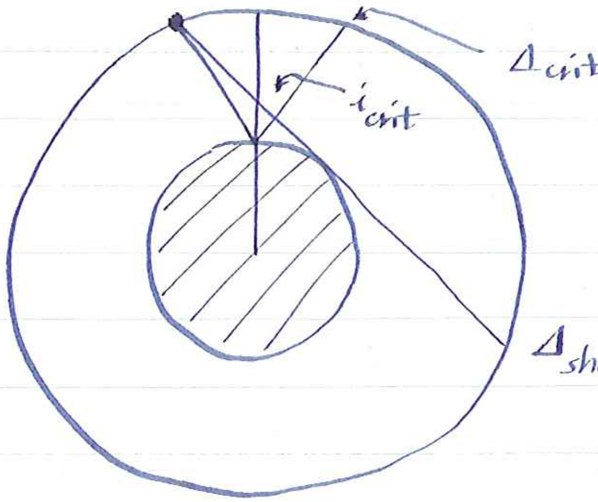

No SKS for $\Delta < \Delta_{crit}$

$\Delta_{crit} \sim$ 62° for ⊕

For $\Delta = \Delta_{crit}$, SKS and ScS coincide. Plot of p vs. Δ thus looks like:

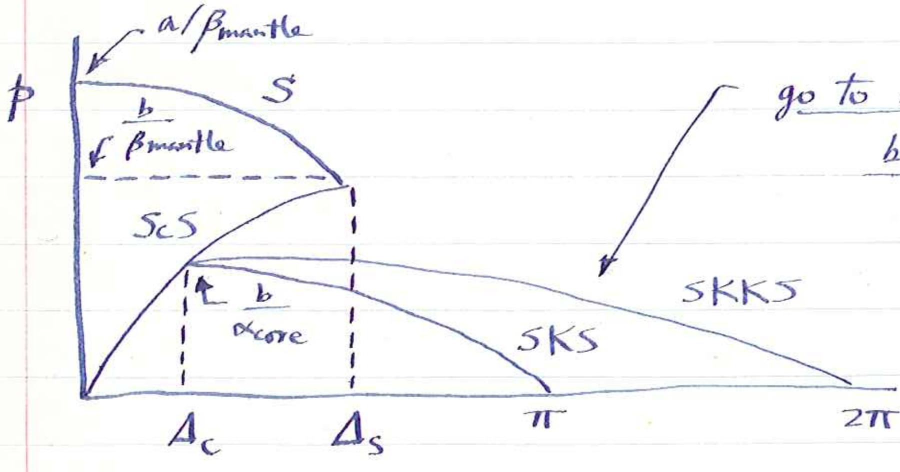

<u>go to next page</u> <u>before</u> drawing SKKS, etc. in this figure and that below

The travel time curve looks like:

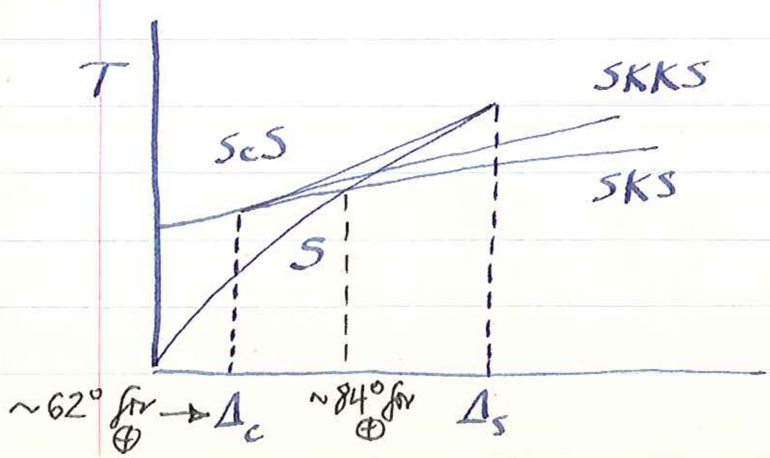

$\Delta \sim 84°$ where S and SKS cross.

What about SKKS, SKKKS, etc?

At any $\Delta > \Delta_{crit}$ $\exists$ an ∞ family of rays SKS, SKKS, etc.

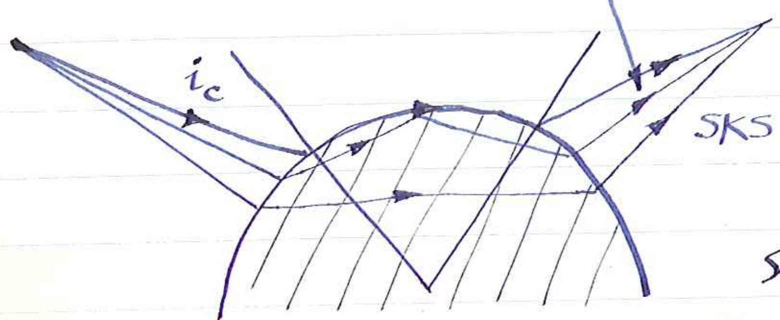

$S\infty KS$ suffers an ∞ no. of internal bounces, travels <u>along</u> core-mantle interface

Similar to the <u>whispering gallery</u> phenomenon in St. Paul's Cathedral, London.

The times of the rays SKKS, SKKKS, etc. approach that of $S\infty KS$ which appears to travel along the core-mantle interface

Geometrical ray theory clearly fails adequately to describe this coalescence of rays.

Ray tracing plot for SKKKS: note small azimuth range leaving source gets spread out considerably, amplitudes of SKKKS etc. thus <u>weak</u>.

S_nKS has $n-1$ caustics

Note <u>caustic surface</u> inside core: locus of crossing points of nearby rays, this surface does <u>not</u> intersect surface of $\oplus$.

Passage of a ray through a caustic gives rise to a <u>$\pi/2$ change in phase</u>.
Reason: consider ray bundle

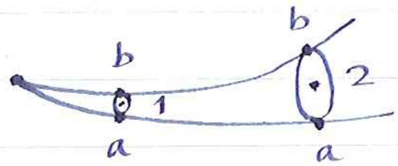

Amplitude law:
$A_2/A_1 \sim (\text{area }1/\text{area }2)^{1/2}$

Caustic surface is where nearby rays <u>cross</u>

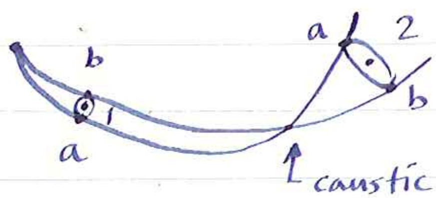

The ray bundle gets turned inside out. The area at 2 is <u>negative</u>.

Thus (this actually just a mnemonic device, not a rigorous derivation):

$$A_2/A_1 = \left(-\left|\frac{\text{area }1}{\text{area }2}\right|\right)^{1/2}$$

$$= i\left|\frac{\text{area }1}{\text{area }2}\right|^{1/2}, \quad i = e^{i\pi/2}$$

a $\pi/2$ <u>phase advance upon passage thru caustic</u>

This not easy to observe with SKKS, SKKKS, etc. since $\exists$ phase shifts at CM bdry as well which depend upon angle i.

But another such situation of an <u>internal caustic</u> is PP, SS etc.

See ray tracing plot for PP; SS would look similar. If attention restricted to SH phase shift upon surface reflection is nil and SS should be phase advanced relative to S by exactly $\pi/2$.

Given a <u>pulse</u> $s(t)$ if every constituent Fourier component is phase shifted uniformly by $\pi/2$ the result is said to be the <u>Hilbert transform</u> of $s(t)$. We may think of passage thru a caustic as a black box which converts $s(t)$ into $H[s(t)]$, its <u>Hilbert transform</u>.

$$\sin\omega t \rightarrow \boxed{\begin{array}{c}\text{Hilbert}\\ \text{transform}\end{array}} \rightarrow \cos\omega t = \sin(\omega t + \tfrac{\pi}{2})$$

Passage thru 2 such boxes advances phase by π, equivalent to multiplication by -1

$$s(t) \rightarrow \boxed{\begin{array}{c}\text{Hilbert}\\ \text{transform}\end{array}} - \boxed{\begin{array}{c}\text{Hilbert}\\ \text{transform}\end{array}} \rightarrow -s(t) = \sin(\omega t + 180^\circ)$$

in the case above

Figs. 9 and 10 from Choy + Richards show two transverse S + SS seismograms.

The Hilbert transform of a seismograph-filtered impulse

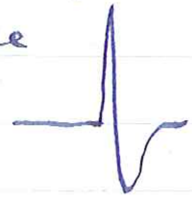

looks like the signal shown, viz.

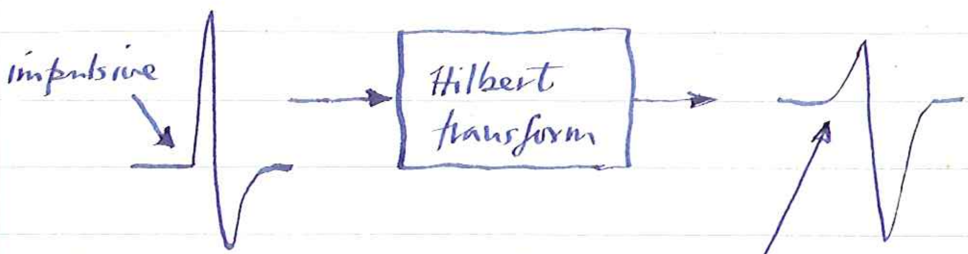

broad downswing

emergent, hard to "pick" first arrival — this associated with fact that SS not a least time path

But Hilbert transformation of the seismogram, accomplished easily in computer, has precisely the expected effect:

1. H[S] takes on the emergent character of SS
2. H[SS] looks like −S, but weaker due to shear attenuation, finite Q_β.

This a particularly clear example of caustic phase shift.

Note that at the caustic itself ray theory predicts an ∞ amplitude

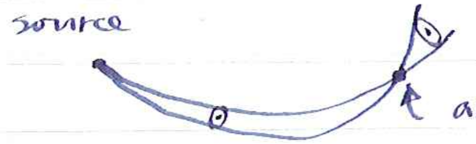

area of ray bundle → zero at caustic

amplitude $\sim 1/\sqrt{\text{area}} \to \infty$

This an example of failure of ray theory, fails near caustics, focal points and shadow boundaries.
At all such locations the finite frequency of the waves must be taken into account.
Above problem does not arise for SS etc. since caustic does not intersect ⊕ surface, but PKP caustic does, at $\Delta \sim 143°$.

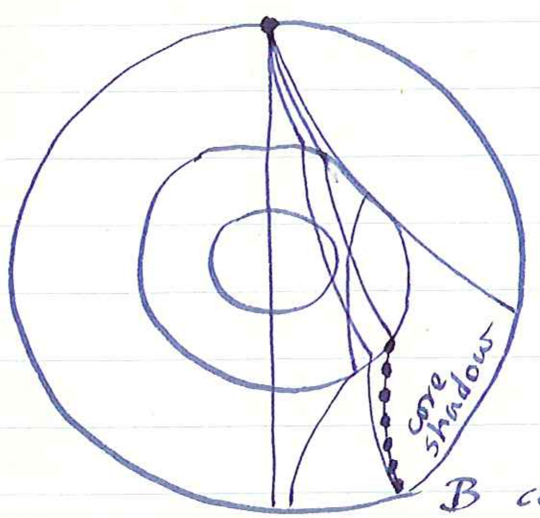

A core shadow $\Delta \sim 105°$

B caustic $\Delta \sim 143°$

F antipode $\Delta = 180°$

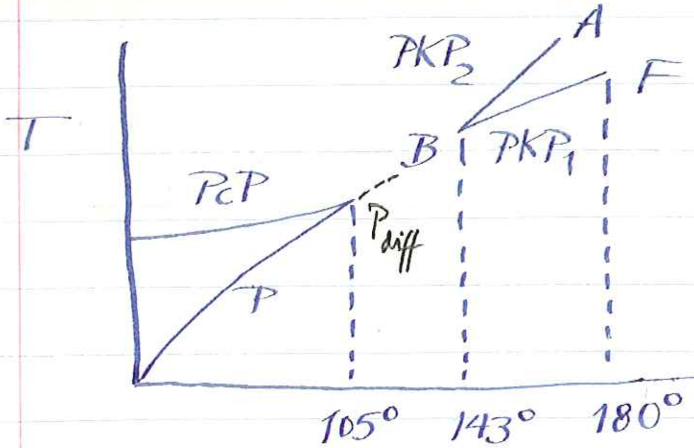

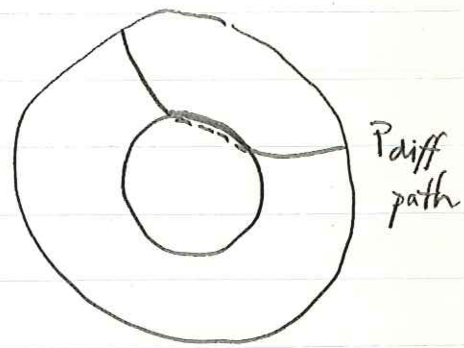

Ray theory predicts ∞ amplitude arrivals at point B, PKP caustic, also predicts <u>sharp</u> shadow bdry at $\Delta \sim 105°$.
Actually <u>diffracted</u> P_{diff} is seen far into the shadow, particularly at long periods.

Amplitude at B is <u>large</u> but not ∞. Theory for behavior of waves in vicinity of caustic due to <u>Airy</u>, whom we have met in connection with isostasy.

An <u>everyday example</u> of <u>caustics</u> : patterns of dark and light on bottom of a swimming pool on sunny day, due to refraction at air-water interface, focusing and defocusing

term "caustic" ⇒ burning, intense

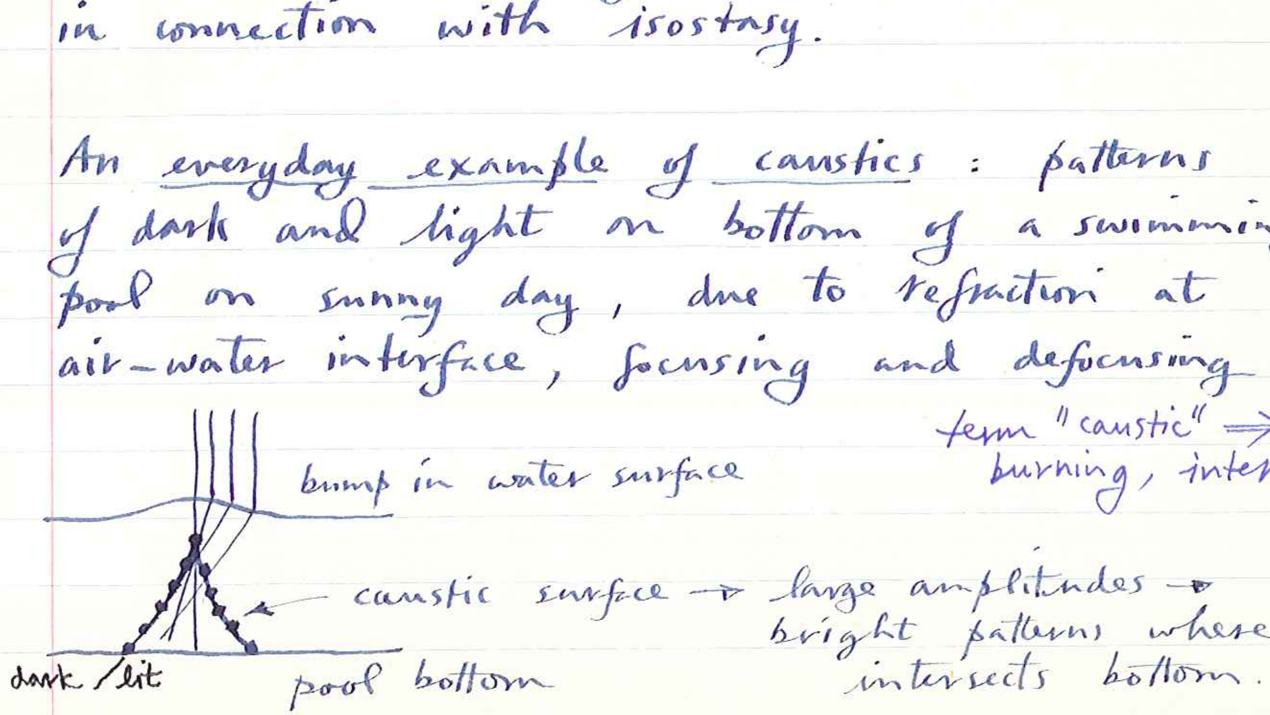

Travel time plot for <u>surface</u> focus shows the various phenomena associated with the <u>core</u> we have been discussing :

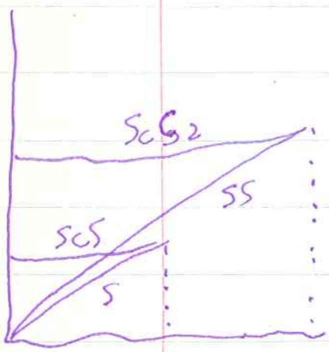

1. P and PcP joining at core shadow, P_{diff} extending way into core shadow, makes it difficult to determine location of shadow boundary
2. PKP_1 and PKP_2 with CD branch (PKiKP) going into core shadow
3. notice also PP, PPP, etc.
4. S and ScS, SKS, SKKS, etc.

All the above are empirical. Many of the phases shown not necessarily observed. Easy to determine expected times of compound phases e.g. PKPPKP by adding relevant segments together

5. LQ and LR, straight lines, constant velocity are approximate arrival times of 20 s period Love and Rayleigh surface waves, dominant signal for oceanic paths, shallow focus events.

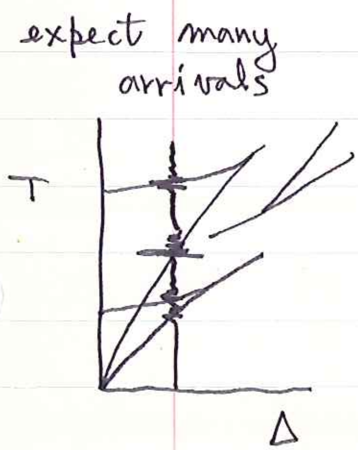

Consider now effect of <u>continuous</u> but <u>rapid</u> changes in velocity.
Also important in $\oplus$, two cases of interest, both occur in <u>upper mantle</u>.

<u>High velocity gradient</u>: similar to S, SKS case. Suppose $v(r)$ looks like

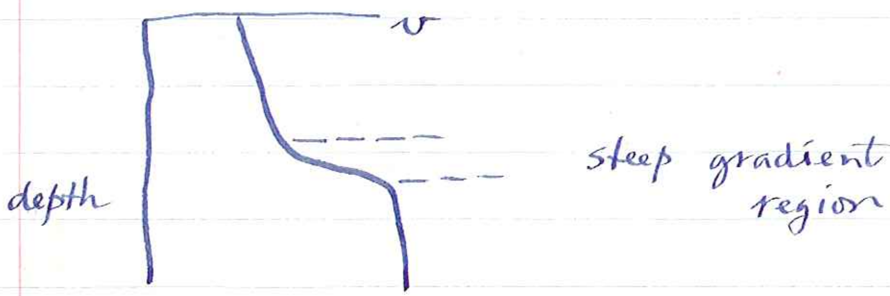

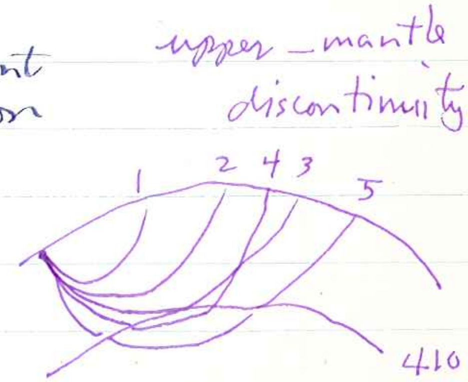

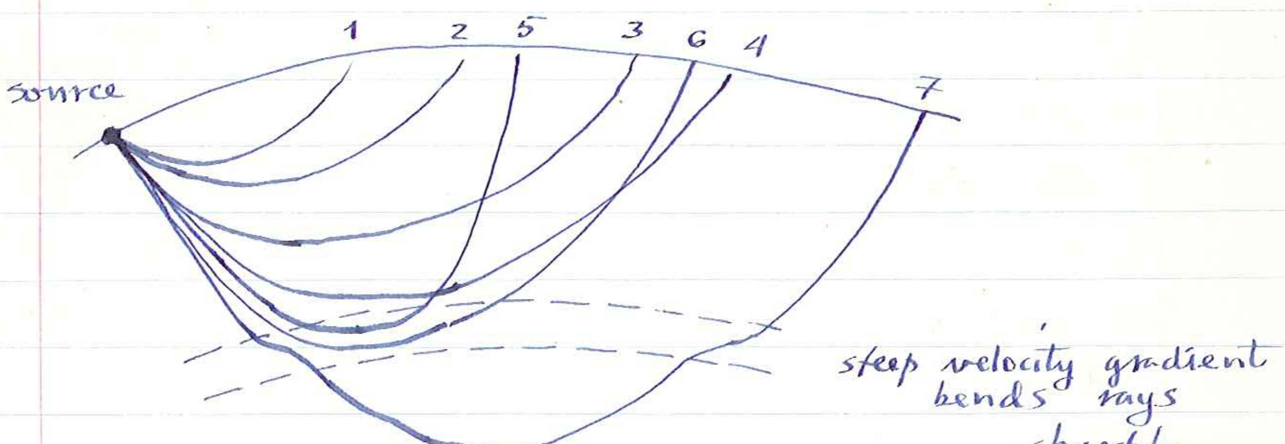

Travel time plot thus looks like: called a <u>triplication</u>.

back branch both dT and $d\Delta$ negative

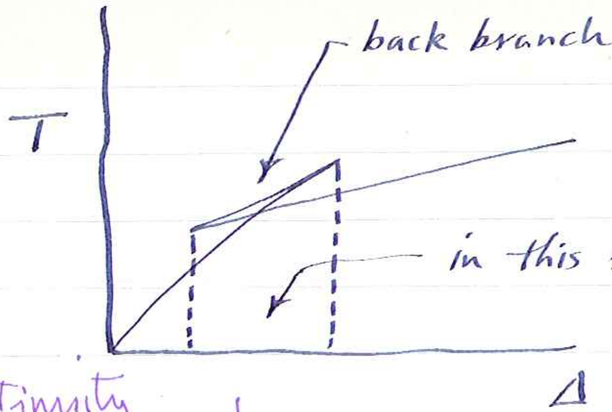

in this range ∃ 3 arrivals, correspond to S, totally reflected ScS and refracted SKS in case of S interaction with core

discontinuity

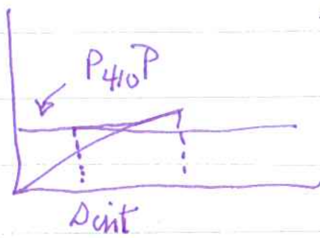

$p(\Delta)$ thus looks like, smooth continuous curve

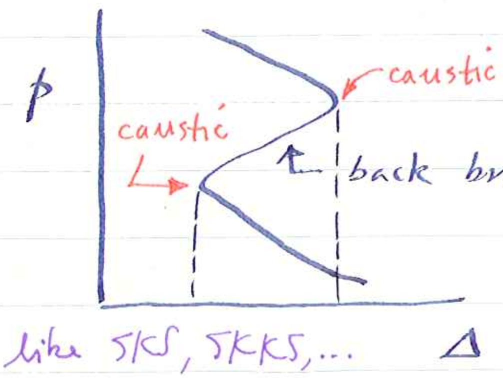

back branch $d\Delta$ negative

like SKS, SKKS, ...

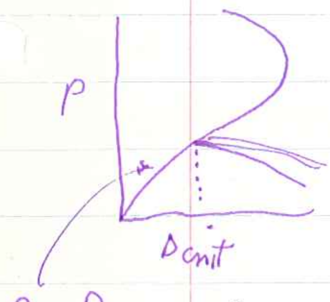

Observed triplications suggest ∃ two major high velocity gradient zones in upper mantle at depths of ~ 410 km and ~ 650 km. Easiest to observe using arrays. Recall Fig. 4 from TFSO study by Lane Johnson, location of epicenters used shown in Fig. 5

One triplication in range $15° \lesssim \Delta \lesssim 20°$ and another in range $20° \lesssim \Delta \lesssim 25°$.

His interpretation CIT 204 shown in Fig. 24, two steep gradient zones at ~400 km and ~650 km depth.

To actually see all three arrivals is not easy. Look at ray tracing diagram for Δ out to $40°$ for model CIT 204 from Julian and Anderson Fig. 25.

Spacing of rays at surface an indication of expected amplitude (if shot out from source in equal solid angles). In general for a triplication it is found that

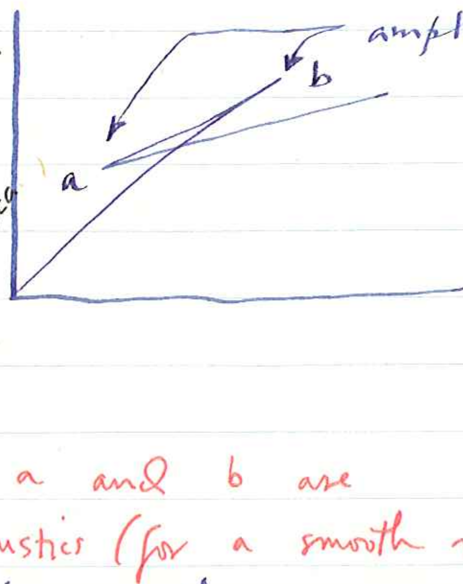

amplitudes largest at point a (corresponds essentially to total internal reflection) next largest at b, weaker between a and b

Look also at Walck & Clayton record section – Scarlet Array – Middle America quakes

Both a and b are caustics (for a smooth $v(r)$); $p(\Delta)$ is smoothly

In fact this another example of failure of vertical ray theory, which predicts that

$$\text{amplitude} \sim (d^2T/d\Delta^2)^{1/2}.$$

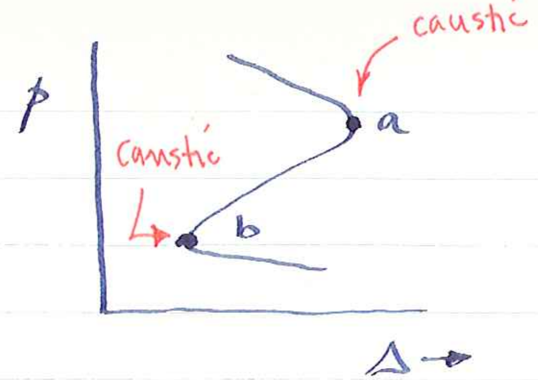

Ray theory predicts ∞ amplitudes at points a and b since $d^2T/d\Delta^2 = dp/d\Delta \to \infty$ (p vs. Δ turns vertical)

For a model

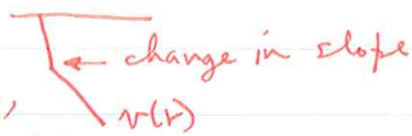

get, instead,

<u>Modern</u> method of studying upper mantle structure is <u>using synthetic seismograms</u>, try to match <u>amplitudes</u> of later arrivals and other details of waveform.

Example of this method : work of Helmberger and Wiggins LRSM stations in western U.S. , nuclear explosions at NTS , Fig. 2 shows two record sections <u>reduced</u> to velocity of 10.8 degrees / second. Large amplitude second arrival in range $\Delta \sim 15° - 20°$ very clear , see e.g. station WNSD from Aardvaark , due to "discontinuity" at 400 km depth.

Fig. 16 shows their suggested refinement of CIT204 (__) , p vs. Δ curve with more structure